ELSEVIER

New isotopic evidence for the origin of groundwater from the Nubian Sandstone Aquifer in the Negev, Israel

Avner Vengosh [a,*], Sharona Hening [b], Jiwchar Ganor [b], Bernhard Mayer [c], Constanze E. Weyhenmeyer [d], Thomas D. Bullen [e], Adina Paytan [f]

[a] *Division of Earth and Ocean Sciences, Nicholas School of the Environment and Earth Sciences, Duke University, Durham, NC 27708, USA*
[b] *Department of Geological and Environmental Sciences, Ben Gurion University, Beer Sheva, Israel*
[c] *Department of Geology and Geophysics, University of Calgary, Calgary, Alberta, Canada*
[d] *Department of Earth Sciences, Syracuse University, Syracuse, NY, USA*
[e] *US Geological Survey, Menlo Park, CA, USA*
[f] *Department of Geological and Environmental Sciences, Stanford University, Stanford, CA, USA*

Abstract

The geochemistry and isotopic composition (H, O, S, $O_{sulfate}$, C, Sr) of groundwater from the Nubian Sandstone (Kurnub Group) aquifer in the Negev, Israel, were investigated in an attempt to reconstruct the origin of the water and solutes, evaluate modes of water–rock interactions, and determine mean residence times of the water. The results indicate multiple recharge events into the Nubian sandstone aquifer characterized by distinctive isotope signatures and deuterium excess values. In the northeastern Negev, groundwater was identified with deuterium excess values of $\sim16\%_0$, which suggests local recharge via unconfined areas of the aquifer in the Negev anticline systems. The $\delta^{18}O_{H_2O}$ and δ^2H values ($-6.5\%_0$ and $-35.4\%_0$) of this groundwater are higher than those of groundwater in the Sinai Peninsula and southern Arava valley ($-7.5\%_0$ and $-48.3\%_0$) that likewise have lower deuterium excess values of $\sim10\%_0$. Based on the geochemical differences between groundwater in the unconfined and confined zones of the aquifer, a conceptual geochemical model for the evolution of the groundwater in the Nubian sandstone aquifer has been reconstructed. The isotopic composition of shallow groundwater from the unconfined zone indicates that during recharge oxidation of pyrite to SO_4 ($\delta^{34}S_{SO_4} \sim-13\%_0$; $\delta^{18}O_{SO_4} \sim+7.7\%_0$) and dissolution of $CaCO_3$ ($^{87}Sr/^{86}Sr \sim0.70787$; $\delta^{13}C_{DIC} = -3.7\%_0$) occur. In the confined zone of the aquifer, bacterial SO_4 reduction removes a significant part of dissolved SO_4^{2-}, thereby modifying its isotopic composition ($\delta^{34}S_{SO_4} \sim-2\%_0$; $\delta^{18}O_{SO_4} \sim+8.5\%_0$) and liberating dissolved inorganic C that contains little or no radiocarbon (^{14}C-free) with low $\delta^{13}C_{DIC}$ values ($<-12\%_0$). In addition to local recharge, the Sr and S isotopic data revealed contribution of external groundwater sources to the Nubian Sandstone aquifer, resulting in further modifications of the groundwater chemical and isotopic signatures. In the northeastern Negev, it is shown that SO_4-rich groundwater from the underlying Jurassic aquifer contributes significantly to the salt budget of the Nubian Sandstone aquifer. The unique chemical and isotopic composition of the Jurassic groundwater ($\delta^{34}S_{SO_4} \sim +14\%_0$; $\delta^{18}O_{SO_4} \sim 14\%_0$; $^{87}Sr/^{86}Sr \sim0.70764$) is interpreted as reflecting dissolution of Late Triassic marine gypsum deposits. In the southern Arava Valley the authors postulate that SO_4-rich groundwater with distinctively high Br/Cl (3×10^{-3}) low $^{87}Sr/^{86}Sr$ (0.70734), and high $\delta^{34}S_{SO_4}$ values ($+15\%_0$)

---

* Corresponding author. Tel.: +1 919 681 8050; fax: +1 919 684 5833.
 E-mail address: vengosh@duke.edu (A. Vengosh).

is derived from mixing with underlying brines from the Paleozoic units. The radiocarbon measurements reveal low ^{14}C activities (0.2–5.8 pmc) in both the northeastern Negev and southern Arava Valley. Taking into account dissolution of carbonate rocks and bacterial SO_4 reduction in the unconfined area, estimated mean residence times of groundwater in the confined zone in the northeastern Negev are on the order of 21–38 ka, which suggests recharge predominantly during the last glacial period. The ^{14}C signal in groundwater from the southern Arava Valley is equally low but due to evidence for mixing with external water sources the residence time estimates are questionable.

1. Introduction

Stable and radioactive isotopes are commonly used in order to study the origin, age and chemical evolution of groundwater. The deuterium excess (d-excess $= \delta^2H - 8\delta^{18}O$) describes the conditions that lead to kinetic isotope fractionation between water and vapor during primary evaporation in the oceans (e.g., Dansgaard, 1964). Deviation from a slope of 8 on a plot of δ^2H versus $\delta^{18}O$ may indicate evaporation, mixing between different water groups, or water–rock interactions. In cases where the slope is equal to 8, the d-excess is commonly used as a characteristic property of the recharge source (e.g., Gat and Issar, 1974). By examining the ^{14}C activity of water, it is sometimes possible to constrain the ages of the recharge events. However, ground–water systems are complex and therefore it is not always possible to constrain the age and sources of the water using only $\delta^{18}O$, δ^2H and ^{14}C tracers. In most cases, the ^{14}C ages are strongly influenced by water–rock interactions. A better understanding of these interactions may be obtained by adding information on the isotopic compositions of the dissolved constituents of the groundwater such as S and Sr isotopes. The advantages of this multi-isotope (O, H, C, S and Sr) approach are demonstrated in the present paper for the case study of the Nubian sandstone aquifer (NSA) in the Negev, Israel.

The scarcity of water resources in arid zones often requires exploitation of "paleo" groundwater that has recharged into the aquifers during earlier geological times (i.e., water that is not participating in the present hydrological cycle). Groundwater in many basins of the NSA across the Sahara and Sahel regions in northern Africa and in the arid zones of the Middle East have low $\delta^{18}O_{H_2O}$, δ^2H, and deuterium-excess values ($\leqslant 10‰$) relative to modern precipitation in these regions (d-excess $>16‰$; Sonntag et al., 1978; Gat, 1981, 1983; Gat and Issar, 1974; Gat and Galai, 1982; Sultan et al., 1997; Levin et al., 1980; Yechieli et al., 1992; Clark and Fritz, 1997). In addition, ground-water from the NSA has typically low ^{14}C activities (Issar et al., 1972). These characteristics have been interpreted as reflecting paleo-recharge during periods of higher humidity during the Late Pleistocene (Issar et al., 1972; Issar, 1981; Gat, 1981; Gat and Issar, 1974; Gat and Galai, 1982).

In the Sinai Peninsula and the Negev (Fig. 1), the NSA is part of the Lower Cretaceous Kurnub Group (Issar et al., 1972). Given that modern precipitation in this area is low (<150 mm annually; Levin et al., 1980), the origin of groundwater in the NSA in the Negev and Arava Valley in Israel has been attributed to northeasterly flow of palaeo-groundwater from the Sinai Peninsula. It has been suggested that most of the recharge to this aquifer occurred through the outcrops of the Lower Cretaceous sandstone in southern Sinai during the last glacial period (Issar et al., 1972; Issar, 1981; Gat and Galai, 1982; Gat and Issar, 1974; Kroitoru, 1980; Yechieli et al., 1992).

In most parts of the NSA, the salinity of the groundwater is low. In the Disi aquifer in southern Jordan, for example, the level of the total dissolved solids (TDS) in most parts of the aquifer does not exceed 500 mg/L (El-Naser and Gedeon, 1996). Likewise, groundwater from the NSA in western Egypt is characterized by low salinity (Puri et al., 2001). However, the salinity of groundwater from the NSA in the Negev and northern Sinai Peninsula is high with TDS ranging from 1000 to 7000 mg/L (Yechieli et al., 1992; Guttman et al., 1999; Burg et al., 1999; Rosenthal et al., 1998; Abed El Samie and Sadek, 2001). Several different explanations have been postulated for the origin of the dissolved constituents in the NSA groundwater of the Negev, including: (1) mixing with relicts of entrapped sea-water that was not sufficiently flushed from the aquifer (Issar, 1981), (2) mixing with Ca–chloride brines (Yechieli et al., 1992; Guttman et al., 1999; Burg et al., 1999), and (3) continuous salt dissolution and water–rock interactions along subsurface groundwater flow from the Sinai Peninsula to the Negev (Rosenthal et al., 1998).
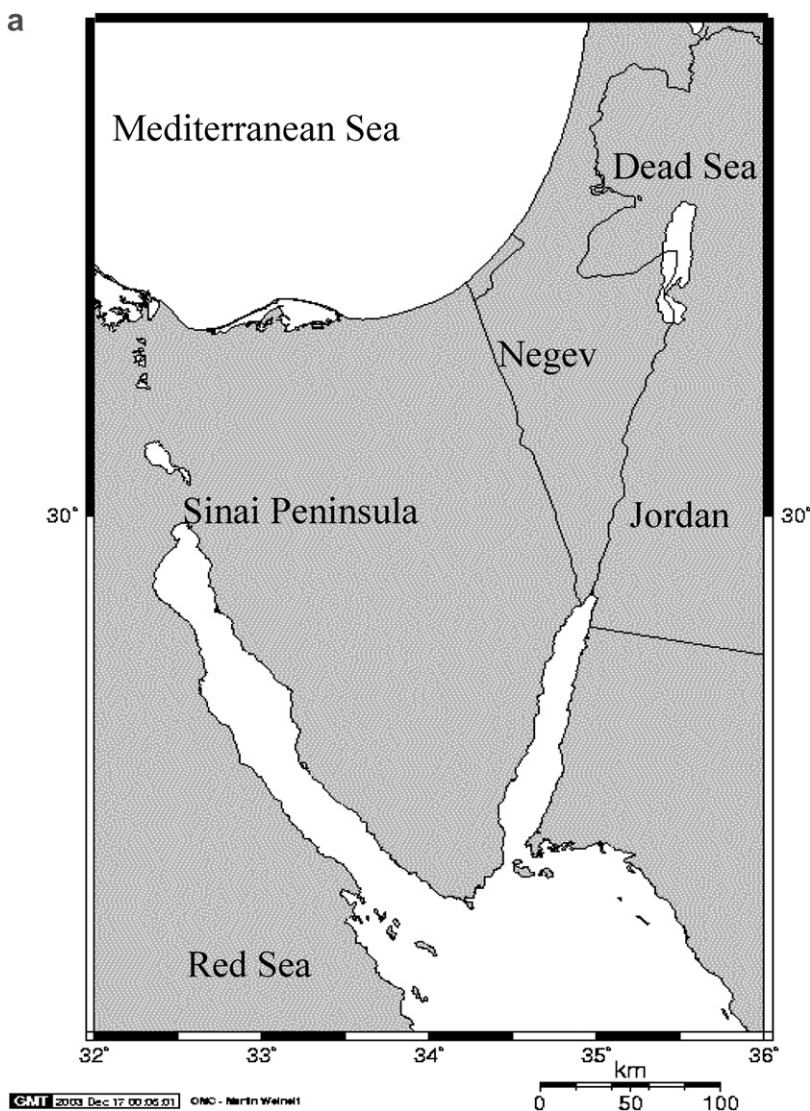
a

Fig. 1. (a) A general map of Sinai Peninsula and the Negev. (b) A location map of sampling wells (M refers to the wells of Makhtesh), major geological structures (doubled arrows), ground water levels (in meters above sea level), and major flow regimes after Guttman et al. (1999) (arrows) in the Negev and Arava Valley (marked as I–III, respectively). Line A–A′ marks the hydrogeological cross section presented in Fig. 2. (c) A detailed location map of wells in the northeastern Negev with the values of the Cl⁻ contents (in mg/L).

The aim of this paper is to evaluate the sources of the water and the dissolved constituents in groundwater from the NSA in the Negev, and to provide isotopic constraints for the existing hydrological models of groundwater migration and evolution. In particular, the questions of recharge, high salinity, and high SO_4^{2-} content that characterize the groundwater from the NSA are addressed. A large suite of groundwater chemical data and isotopic tracers that include O in water and sulfates ($\delta^{18}O_{H_2O}$, $\delta^{18}O_{SO_4}$), H (δ^2H), S ($\delta^{34}S_{SO_4}$), C ($\delta^{13}C_{DIC}$, ^{14}C), and Sr ($^{87}Sr/^{86}Sr$) are used. It is

demonstrated that an integration of a large suite of geochemical and isotopic tracers can be a powerful tool for delineating the origin of groundwater in a complex system like the NSA. The different isotopic tracers are used to identify different recharge regimes, mechanisms of water–rock interactions, external groundwater sources that flow to the NSA, and factors that affect the ^{14}C activity of groundwater. The application of the proxies utilized for this study could be used for other NSA basins in the Middle East and possibly other aquifers worldwide.
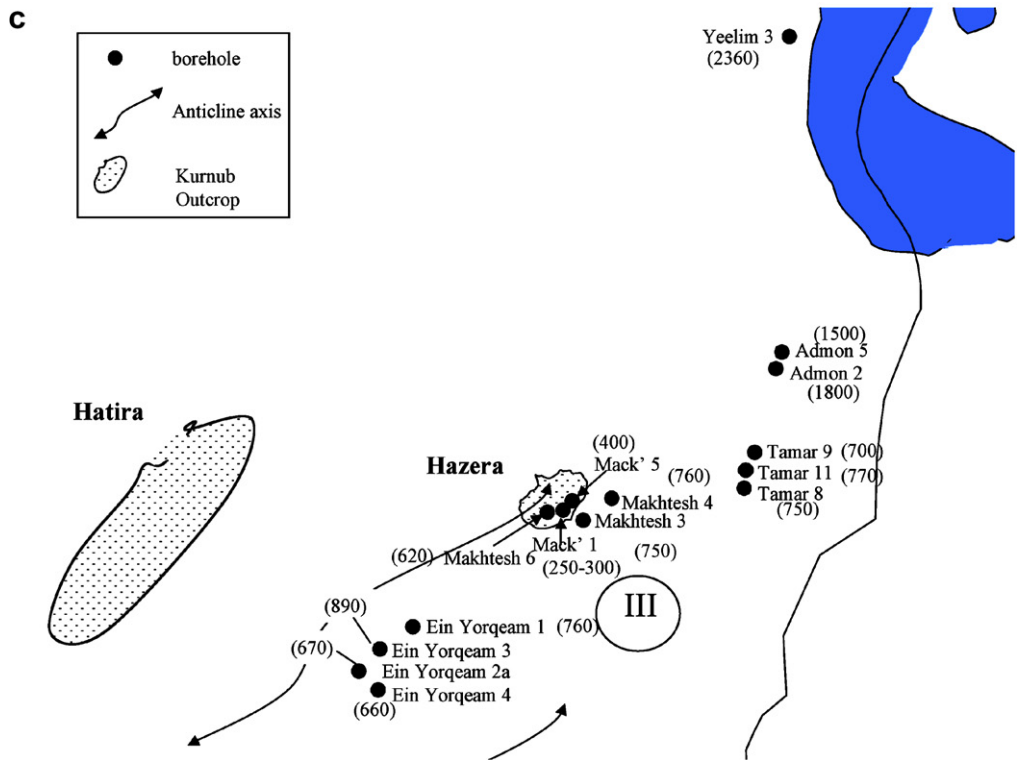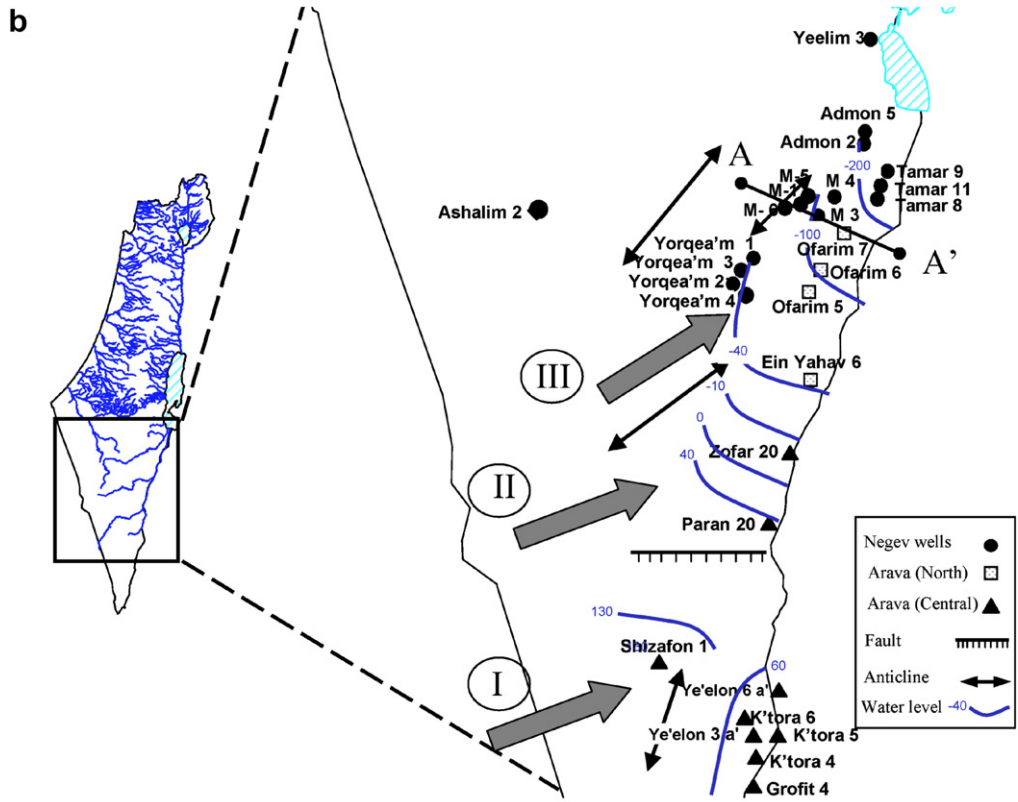
b

c

Fig. 1 (*continued*)

2. Hydrogeological background

The Nubian Sandstone Aquifer (NSA) is part of the massive Paleozoic to Lower Cretaceous sedimentary sequence that constitutes the major aquifer units in the Middle East and northern and eastern Africa. In the study area, the NSA is represented by the Lower Cretaceous Kurnub Group, which is composed of alternating beds of sandstone and shale. The Kurnub Group is exposed at the margins of the igneous massif in southern Sinai and along the major anticline structures of the Negev (Fig. 1). In the northern Negev the NSA overlies Jurassic aquifers. In the northwestern Negev, the underlying Jurassic aquifers are confined by impermeable layers (Kidod Formation), which do not exist in the northeastern Negev (Rosenthal et al., 1981; Weinberger and Rosenthal, 1994). Consequently, a direct hydrological contact exists between the NSA and underlying Jurassic units in the northeastern Negev (Nativ et al., 1987). In the southern Negev and southern Arava Valley, the NSA overlies and is hydraulically connected with the underlying Paleozoic units (Nativ et al., 1987). Specific details on the aquifer lithology and the hydrogeological background are given in Kroitoru (1980), Nativ et al. (1987), Rosenthal et al. (1990, 1992), Weinberger and Rosenthal (1994), Weinberger et al. (1991), Guttman et al. (1999) and Burg et al. (1999).

Fig. 2 illustrates a cross section from the unconfined area in the vicinity of one of the anticlines (Makhtesh Qatan) in the west to the confined area of the NSA and the eastern margin of the NSA along the major faults of the Dead Sea Rift Valley. The underlying Jurassic aquifer is accessed by the Makhtesh 6 well (M6) in the vicinity of Makhtesh Qatan anticline.

In the eastern Negev and Arava Valley, Guttman et al. (1999) defined several flow regimes for the eastern Negev and Arava Valley (marked as I–III in Fig. 1b). The flow regimes are controlled by the NE–SW asymmetrical anticlines that characterize the northern and central Negev, in which the NSA is exposed in erosion cirques that are associated with the major anticlines ("makhteshim"). The flow patterns are also controlled by the fault systems. Along the Dead Sea – Arava Rift Valley, the major faults divert the flow and act as the eastern boundary of the aquifer. In the southern Arava Valley and Negev, E–W faults also affect the flow lines. In general, the water gradients in the Negev follow the major geological structures with SW–NE flow (Fig. 1b). In the southern Arava Valley the flow gradient is north to south (Burg et al., 1999).

Groundwater from the NSA is highly mineralized with TDS ranging from 1000 mg/L in southern Sinai Peninsula to about 7000 mg/L in the northern and eastern Negev (Yechieli et al., 1992; Rosenthal et al., 1992; Burg et al., 1999; Guttman et al., 1999). Kroitoru (1980) recognized that the groundwater salinity progressively increases along flow paths towards the northwestern and northeastern Negev. This increase in salinity has been attributed to changes in lithology and a higher clay fraction that reduces the permeability and thus the flushing of entrapped saline groundwater (Kroitoru, 1980).
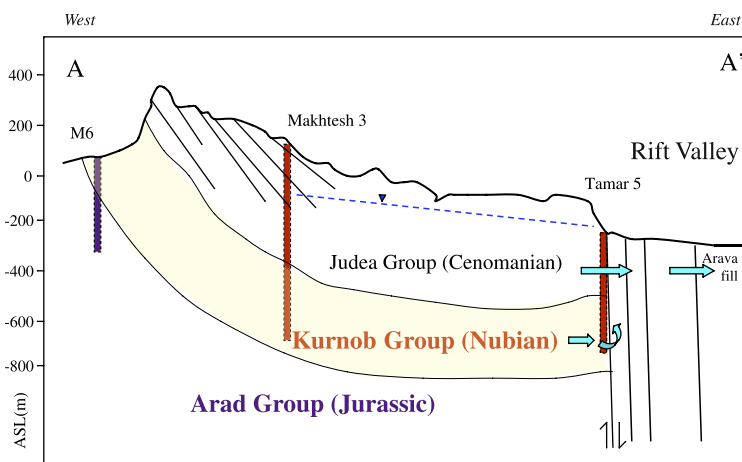

Fig. 2. A schematic hydrogeological cross section from Makhtesh Qatan anticline in the west to the Rift Valley in the east (line A–A′ in Fig. 1; modified from Rosenthal et al., 1981).

3. Sampling and analytical techniques

Groundwater samples were collected from 30 wells in the Negev and Arava Valley between 2001 and 2003. Water samples were collected from active pumping wells and were initially preserved in a cold box and later transferred to a refrigerator in the laboratory. Field work included measurements of temperature, pH, and conductivity. Water samples were filtered immediately upon reaching the laboratory. Cations and B concentrations were determined by inductively coupled plasma-optical emission spectrometry (ICP-OES), Cl^- and HCO_3^- by titration, and Br^-, NO_3^- and SO_4^{2-} by ion chromatography (IC). Charge balance calculations showed that charge imbalance did not exceed 5%.

Stable isotope ratios are reported in parts per thousand (‰) using the conventional delta notation:

$$\delta_{sample}(‰) = [(R_{sample} - R_{standard})/R_{standard}] \times 1000 \tag{1}$$

where R represents the $^{34}S/^{32}S$, $^{18}O/^{16}O$, $^{2}H/^{1}H$ or $^{13}C/^{12}C$ ratios of the samples and the standards, respectively. Oxygen and H isotope ratios of water were determined at CSIRO, Adelaide, Australia using a standard CO_2 equilibration technique for O and the Zn reduction method for H. The precisions of measurements are $\pm 0.1‰$ and $\pm 0.3‰$, respectively, and results are reported relative to Vienna Standard Mean Ocean Water (V-SMOW). Strontium was separated through ion-exchange using Biorad AG50X8 resin at Ben-Gurion University and the isotopic ratios were measured by thermal ionization mass-spectrometry at the US Geological Survey, Menlo Park, California, USA. An external precision of 2×10^{-5} for the Sr isotope measurements was determined by replicate analyses of the N.I.S.T. 987 standard. Laboratory preparation and mass spectrometry procedures are identical to those described in Bullen et al. (1996).

Sulfate in groundwater was extracted by anion exchange resins (Biorad AG-1X8) at Ben Gurion University and shipped to the University of Calgary (Canada) for determination of S and O isotope ratios. Sulfate was quantitatively recovered from the resin with 15 mL of 3 M HCl, and $BaSO_4$ was precipitated by adding 5 mL of 0.2 M $BaCl_2$ to solution. The precipitate was recovered by filtration, carefully washed with distilled water, and dried prior to isotope analyses. Sulfur isotope analyses were performed by continuous flow isotope ratio mass spectrometry (e.g., Giesemann et al., 1994).

For O isotope analyses on SO_4^{2-}, $BaSO_4$–oxygen was converted to CO at 1450 °C in a pyrolysis reactor (Finnigan TC/EA). The resultant gas was subsequently carried by a He stream into a mass spectrometer for isotope ratio determinations in continuous-flow mode (CF-IRMS). $\delta^{34}S$ values are reported relative to Canon Diablo Troilite (CDT) and $\delta^{18}O$ values relative to Vienna Standard Mean Ocean Water (V-SMOW). Two international reference materials, NBS-127 and OGS, as well as several lab-internal standards were repeatedly measured to ensure accuracy. Reproducibility is $\pm 0.3‰$ for $\delta^{34}S$ measurements and $\pm 0.5‰$ for $\delta^{18}O$ measurements on SO_4.

Carbon isotope ratios ($^{13}C/^{12}C$) and radiocarbon (^{14}C) were measured at the Lawrence Livermore National Laboratory (LLNL), California. Water samples were collected and preserved without any atmospheric contact. For sample preparation, the total inorganic C dissolved in groundwater (DIC) was transformed into CO_2 by acidifying the samples with H_3PO_4 and extracting the liberated CO_2 gas using a standard vacuum extraction line with continuous N_2 flow (McCrea, 1950; Friedman and O'Neil, 1977). The CO_2 gas was split into two sub-samples for $\delta^{13}C$ and ^{14}C measurements. $\delta^{13}C$ measurements were carried out on a VG Prism II isotope ratio mass spectrometer with a precision of $\pm 0.1‰$. For ^{14}C measurements CO_2 was converted into graphite and then analyzed on a 10 MV Tandem Van de Graaff Accelerator at LLN (Vogel et al., 1987; Davis et al., 1990; Southon et al., 1990, 1992; Kirner et al., 1995). Results are given in the standard notation as percent modern carbon (pmc). The reproducibility is generally better than $\pm 0.1\%$.

4. Results

The chemical and isotopic compositions of groundwater from the NSA in the Negev and Arava Valley are presented in Tables 1 and 2, respectively. The results and discussion in the paper are focused on only two geographical areas that reflect different flow zones in the NSA: the southern flow regime I referred to as "Southern Arava Valley" and the northern flow regime (marked as III in Fig. 1b) referred to as "Northeastern Negev". The results for groundwater of the "Northern Arava Valley" (marked as "II") are not discussed in this article.

Table 1
Chemical compositions and field data of groundwater sampled from the Nubian Sandstone aquifer in the Negev

No.	Name	Date	Depth (m)	pH	Temperature	Ca	Mg	Na	K	Cl	SO$_4$	HCO$_3$	Br	Br	Sr	SI
	Northeastern Negev – flow regime III															
	Unconfined aquifer (Group III-A)															
NB-10	Makhtesh 1	06.05.01	214	6.4	28.7	5.39	2.95	10.64	0.55	9.19	9.33	1.77	0.004	0.052	0.012	−0.91
NB-45	Makhtesh 1	28.08.02	214	–	–	3.52	2.36	7.31	0.43	6.46	6.40	1.94	0.002	0.050	0.010	–
Ni-2	Makhtesh 1	04.08.03	214	7.2	28.1	4.67	2.69	8.23	0.44	7.30	6.91	1.80	0.003	0.047	0.011	1.62
Ni-1	Makhtesh 5	04.08.03	287	6.6	29.8	6.26	3.57	13.63	0.75	11.28	9.98	1.84	0.005	0.067	0.017	1.92
	Confined aquifer (Group III-B)															
NB-11	Makhtesh 3	06.05.01	709	7.0	37.7	3.79	2.55	19.77	0.73	21.38	4.27	5.20	0.023	0.091	0.022	0.14
NB-46	Makhtesh 3	13.08.02	709	–	–	3.12	2.72	20.17	0.70	21.51	4.21	3.72	0.022	0.097	0.022	–
Ni-8	Makhtesh 3	04.08.03	709	7.4	37.0	3.67	2.86	20.90	0.66	20.94	3.82	5.53	0.021	0.107	0.024	1.61
NB-12	Makhtesh 4A	06.05.01	800	7.4	35.0	5.04	3.07	20.17	0.84	21.47	6.82	4.96	0.020	0.086	0.021	0.56
NB-47	Makhtesh 4A	28.08.02	800	–	–	4.89	3.30	20.11	0.65	21.36	6.73	4.53	0.021	0.081	0.023	–
Ni-4	Makhtesh 4A	04.08.03	800	8.3	37.9	5.25	3.37	19.64	0.78	22.30	6.10	4.83	0.020	0.093	0.024	−0.40
NB-14	Ein Yorqe'am 1	06.05.01	819	6.9	38.0	3.97	2.76	18.96	0.68	21.18	4.38	5.32	0.020	0.089	0.021	0.07
NB-44	Ein Yorqe'am 1	27.06.02	819	7.5	34.0	2.20	2.18	16.87	0.69	15.77	3.46	3.13	0.020	0.091	0.019	−0.37
Ni-6	Ein Yorqe'am 1	04.08.03	819	8.7	34.2	3.38	2.82	19.00	0.71	22.18	3.97	4.17	0.021	0.097	0.025	−1.13
NB-15	Ein Yorqe'am 2A	06.05.01	850	7.2	37.2	3.77	2.51	17.21	0.65	18.82	3.91	4.95	0.019	0.075	0.021	0.28
NB-49	Ein Yorqe'am 2A	13.08.02	850	–	–	3.66	2.76	16.31	0.57	18.43	3.87	4.91	0.019	0.082	0.023	–
Ni-5	Ein Yorqe'am 2A	04.08.03	850	8.1	37.1	3.88	2.62	16.30	0.66	19.06	3.63	5.28	0.018	0.086	0.023	−0.40
NB-43	Ein Yorqe'am 3	27.06.02	855	6.3	34.9	4.94	4.01	21.36	0.58	24.79	4.79	5.49	0.026	0.083	0.027	0.22
NB-50	Ein Yorqe'am 3	13.08.02	855	–	–	5.11	3.81	21.38	0.60	25.38	5.18	5.48	0.025	0.088	0.031	–
NB-51	Ein Yorke'am 4	13.08.02	759	–	–	3.22	2.87	16.91	0.53	17.97	3.66	4.20	0.019	0.079	0.022	–
Ni-7	Ein Yorqe'am 4	04.08.03	759	7.5	37.0	3.62	2.83	17.10	0.50	18.97	3.42	5.21	0.017	0.078	0.021	0.27
	Confined aquifer along the eastern margin (Group III-C)															
NB-8	Tamar 9	26.2.01	450	7.2	39.2	3.70	2.69	16.88	1.31	19.01	4.73	4.76	0.019	0.081	0.018	0.26
NB-41	Tamar 9	12.06.02	450	7.3	38.5	4.22	3.63	17.75	0.54	18.73	4.43	4.95	0.016	0.085	0.018	0.50
Ni-32	Tamar 9	11/19/2003	450	6.1	35.5	4.15	2.53	19.35	0.66	21.03	4.21	4.80	0.020	0.095	0.022	–
NB-9	Tamar 11	26.2.01	–	7.0	39.5	7.55	3.38	21.88	1.46	21.38	10.77	4.64	0.021	0.105	0.026	0.34
Ni-39	Tamar 11	11/26/2003	–	6.2	37.6	7.65	3.59	22.00	1.03	21.69	9.65	4.63	0.021	0.122	0.035	1.01
Ni-40	Tamar 8	11/26/2003	–	6.8	39.8	6.56	3.04	19.79	0.95	21.26	7.25	4.52	0.024	0.102	0.030	0.58
NB-2	Admon 5	26.2.01	535	6.1	38.8	8.75	4.46	41.15	1.43	42.79	12.51	4.67	0.048	0.109	0.038	−0.64
Ni-42	Adamon 2	11/26/2003	145	6.5	34.0	6.65	4.56	48.14	1.67	52.41	8.22	5.30	0.073	0.248	0.044	−0.50
NB-34	Yeelim 3	12.06.02	470	7.1	35.3	15.57	5.47	60.03	1.72	66.48	19.46	4.43	0.093	0.196	0.060	0.49
	Jurassic aquifer															
NB-13	Makhtesh 6	06.05.01	657	6.7	–	10.82	2.61	17.13	0.99	17.23	13.45	4.18	0.022	0.075	0.025	–
Ni-3	Makhtesh 6	04.08.03	657	7.1	35.8	11.53	2.91	16.31	0.94	17.71	11.99	3.72	0.022	0.087	0.029	1.95
	Central Arava (flow regime I)															
NB-18	Paran 20	29.10.01	1536	7.0	54.0	7.03	3.72	13.58	0.94	21.13	6.01	3.70	0.048	0.042	0.039	0.43
NB-57	Paran 20	14.10.02	1536	–	–	6.82	3.71	13.64	0.69	21.37	6.41	3.60	0.055	0.044	0.033	–
NB-19	Ye'elon 6A	29.10.01	791	7.2	38.8	2.27	2.07	5.29	0.24	6.96	1.59	4.18	0.009	0.016	0.010	0.13
Ni-17	Ye'elon 6A	8/18/2003	791	9.3	38.8	2.28	2.27	5.38	0.23	7.49	1.63	4.52	0.015	0.016	0.010	0.04
NB-20	Grofit 4	29.10.01	388	7.1	30.4	6.95	4.31	12.98	0.54	21.36	5.66	3.89	0.051	0.032	0.037	0.20
Ni-21	Grofit 4	8/18/2003	388	8.9	31.3	6.14	4.41	14.23	0.47	20.14	6.09	4.38	0.046	0.036	0.034	−0.09
NB-23	ktora 5	29.10.01	473	7.0	33.0	5.64	3.64	9.81	0.40	16.97	3.85	4.07	0.036	0.024	0.027	–
Ni-18	Ktora 5	8/18/2003	473	5.9	33.4	5.19	3.66	10.79	0.31	16.75	4.16	4.50	0.042	0.027	0.023	0.01
Ni-24	Ketora 4	8/18/2003	450	9.1	31.3	4.26	3.35	10.04	0.49	12.29	4.92	4.59	0.016	0.037	0.029	−0.18
Ni-25	Ketora 6	8/18/2003	422	9.4	34.8	7.17	5.12	13.28	0.85	15.77	8.93	6.38	0.019	0.054	0.048	−0.36
NB-24	Shizafon 1	29.10.01	960	6.8	48.9	8.29	4.31	13.50	1.05	17.11	9.30	3.63	0.019	0.041	0.051	0.16
Ni-45	Shizafon 1	4/1/2004	960	6.5	48.2	8.29	6.60	27.96	2.66	17.06	0.00	0.00	0.000	0.046	0.034	2.31
NB-26	Ye'elon 3A	29.10.01	399	6.8	33.7	6.32	3.91	13.25	0.83	18.98	5.95	3.55	0.026	0.032	0.038	–
Ni-20	Ye'elon 3A	8/18/2003	399	8.5	34.3	5.88	3.79	15.11	0.70	19.19	6.56	3.82	0.032	0.037	0.033	0.20
NB-27	Zofar 20	29.10.01	1017	7.1	27.8	23.68	8.28	50.46	2.02	95.28	6.72	0.96	0.368	0.110	0.148	−0.01
Ni-12	Zofar 20	8/12/2003	1017	8.5	35.3	23.48	6.89	53.98	1.98	102.56	6.10	0.00	0.349	0.105	0.114	–

Data for chemical concentrations are reported in mM unit. SI values are Saturation Index for calcite calculated by geochemical code NETPATH 2.0 Plummer et al. (1994).

Table 2
Isotopic compositions of groundwater sampled from the Nubian Sandstone aquifer in the Negev

No	Name	Date	$\delta^{18}O$ (‰)	$\delta^{2}H$ (‰)	d-Excess (‰)	$\delta^{34}S_{SO_4}$ (‰)	$\delta^{18}O_{SO_4}$ (‰)	$^{87}Sr/^{86}Sr$	^{14}C (pmc)	$\delta^{13}C$ (‰)
	Northeastern Negev – flow regime III									
	Unconfined aquifer (Group III-A)									
NB-10	Makhteshh 1	6.5.01	−5.60	−32.1	12.7	–	–	0.70787	–	–
Ni-2	Makhtesh 1	04.08.03	–	–	–	−13.6	7.6	–	67.7	−3.75
Ni-1	Makhtesh 5	04.08.03	–	–	–	−13.4	7.7	–	–	–
	Confined aquifer (Group III-B)									
NB-11	Makhtesh 3	6.5.01	−6.59	−36.2	16.5			0.70779		
Ni-8	Makhtesh 3	04.08.03	–	–	–	0.5	8.2	–	1.2	−8.83
NB-12	Makhtesh 4A	6.5.01	−6.74	−40.1	13.8	–	–	0.70777	–	–
Ni-4	Makhtesh 4A	04.08.03				−1.9	8.5		2.3	−7.80
NB-14	Ein Yorqe'am 1	6.5.01	−6.41	−33.7	17.6	–	–	0.70777	–	–
NB-44	Ein Yorqe'am 1	27.06.02	−6.62	−35.1	17.9	–	–	0.70774	–	–
Ni-6	Ein Yorqe'am 1	04.08.03	–	–	–	−0.3	8.6	–	0.4	−7.26
NB-15	Ein Yorqe'am 2A	6.5.01	−6.49	−34.3	17.6			0.70775		
Ni-5	Ein Yorqe'am 2A	04.08.03	–	–	–	0.1	8.3	–	0.2	−8.69
NB-43	Ein Yorqe'am 3	27.06.02	−6.32	−33.0	17.6			0.70777		
Ni-7	Ein Yorqe'am 4	04.08.03	–	–	–	0.3	9.4	–	–	–
	Confined aquifer along the eastern margin (Group III-C)									
NB-8	Tamar 9	26.2.01	−6.75	−36.0	18.0	–	–	0.70775	–	–
NB-41	Tamar 9	12.06.02	−6.65	−37.5	15.7	–	–	0.70776	–	–
Ni-32	Tamar 9	11/19/2003	–	–	–	3.1	9.4	–	–	–
NB-9	Tamar 11	26.2.01	−7.50	−46.4	13.6	–	–	0.70773	–	–
Ni-39	Tamar 11	11/26/2003	–	–	–	7.2	12.7	–	–	–
Ni-40	Tamar 8	11/26/2003	–	–	–	8.7	12.4	–	–	–
NB-2	Admon 5	26.2.01	−7.62	−49.2	11.8	–	–	0.70764	–	–
Ni-42	Adamon 2	11/26/2003	–	–	–	4.1	10.6	–	–	–
NB-34	Yeelim 3	12.06.02	−7.02	−48.5	7.7	7.7	14.1	0.70758	–	–
Ni-65	Yeelim 1	7/30/2004	–	–	–	19.8	15.9	–	–	–
	Jurassic aquifer									
NB-13	Makhtesh 6	6.5.01	−7.83	−50.5	12.1			0.70764		
Ni-3	Makhtesh 6	04.08.03	–	–	–	15.4	14.4	–	1.5	−7.72
	Central Arava (flow regime I)									
NB-18	Paran 20	29.10.01	−7.83	−52.9	9.7	–	–	0.70739	–	–
NB-19	Ye'elon 6A	29.10.01	−5.73	−27.6	18.2	–	–	0.70778	–	–
Ni-17	Ye'elon 6A	8/18/2003	–	–	–	−0.5	9.7	–	2.9	−7.18
NB-20	Grofit 4	29.10.01	−7.25	−48.4	9.6			0.70734		
Ni-21	Grofit 4	8/18/2003	–	–	–	6.9	10.7	–	0.6	−6.69
NB-23	ktora 5	29.10.01	−6.60	−37.8	15.0	–	–	0.70734	–	–
Ni-18	Ktora 5	8/18/2003	–	–	–	6.4	11.4	–	5.8	−7.87
Ni-24	Ketora 4	8/18/2003	–	–	–	5.2	10.6	–	–	–
Ni-25	Ketora 6	8/18/2003	–	–	–	9.4	11.0	–	–	–
NB-24	Shizafon 1	29.10.01	−8.62	−58.5	10.5	–	–	0.70733	–	–
Ni-45	Shizafon 1	4/1/2004	–	–	–	11.3	12.5	–	–	–
NB-26	Ye'elon 3A	29.10.01	−8.39	−58.2	8.9	–	–	0.70738	–	–
Ni-20	Ye'elon 3A	8/18/2003	–	–	–	6.1	10.8	–	1.0	−6.68
NB-27	Zofar 20	29.10.01	−7.84	−54.7	8.0	–	–	0.70791	–	–
Ni-12	Zofar 20	8/12/2003	–	–	–	14.2	10.7	–	–	–

4.1. The Northeastern Negev – flow regime III

The chemical and isotopic characteristics of the investigated groundwater samples varied widely (Table 1) and were used to group the samples into several categories. Water grouping was based on aquifer setting (i.e., unconfined versus confined) and geographical distribution. Geochemical distinc-

tions were also used by determining the relationships between Cl^- and Br^- contents (Fig. 3), $\delta^{18}O_{H_2O}$ and δ^2H values (Fig. 4), and $\delta^{34}S_{SO_4}$ and
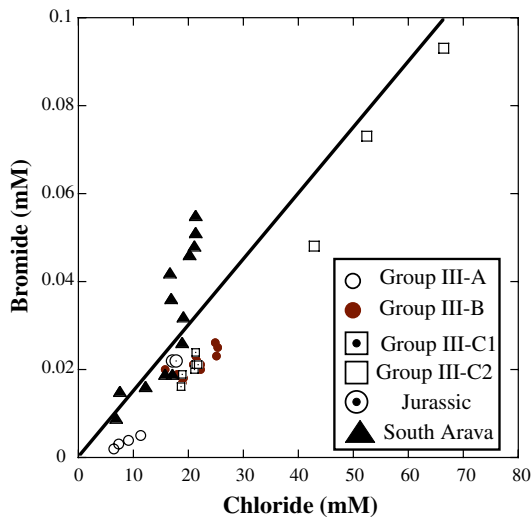

Fig. 3. Bromide versus Cl^- of groundwater from the NSA in the northeastern Negev (Groups III-A, III-B, III-C), Southern Arava Valley (Group I), and underlying Jurassic aquifer. Note the distinction between groundwater from the unconfined zone (Group III-A), confined zone (Group III-B), and eastern section of the aquifer (Group III-C). The line represents seawater Br/Cl ratio ($\sim 1.5 \times 10^{-3}$).
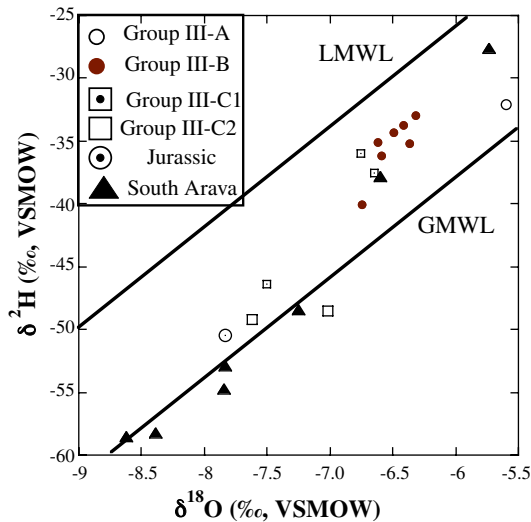
Fig. 4. δ^2H versus $\delta^{18}O_{H_2O}$ values of groundwater from the NSA in the northeastern Negev (circles and squares) and Arava Valley (triangles). GMWL and LMWL represent global and local (eastern Mediterranean) meteoric lines, respectively. Note the distinction between groundwater from the unconfined zone (Group III-A), confined zone (Group III-B) with a slope ~ 8 and relatively high δ^2H and $\delta^{18}O_{H_2O}$ values, and eastern section of the aquifer (Group C) with lower δ^2H and $\delta^{18}O_{H_2O}$ values.

SO_4^{2-} concentrations (Fig. 5). The observations suggest that there are three major types of groundwater in the NSA in the northeastern Negev (Table 1): (1) shallow, low-saline, high $\delta^{18}O_{H_2O}$, and high SO_4^{2-} groundwater from the unconfined part of the aquifer referred to as *Group III-A*; (2) groundwater in the deep and confined area of the NSA with lower $\delta^{18}O_{H_2O}$ and SO_4^{2-} concentrations (*Group III-B*); and (3) groundwater with much lower $\delta^{18}O_{H_2O}$ values and high SO_4 and Cl contents from the eastern part of the aquifer adjacent to the Rift Valley faults (*Group III-C*). The three different water-type groups have distinct chemical and isotope compositions that are described below, and the three groups terminology is used throughout the article.

4.1.1. Group III-A

Groundwater samples that represent the unconfined part of the NSA in the northeastern Negev (Makhtesh 1 and Makhtesh 5 wells) and are characterized by relatively low Cl content (6.5–11.3 mM) and Br/Cl ratio (3×10^{-4}), high SO_4^{2-} (6.4–10 mM)
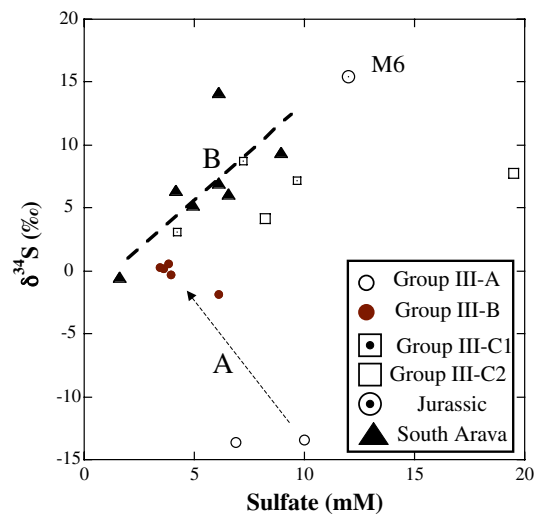
Fig. 5. $\delta^{34}S_{SO_4}$ values versus SO_4^{2-} contents (mmol/L) in groundwater from the NSA in the northeastern Negev (circles and squares) and Arava Valley (triangles). Arrow A represents possible evolution from the recharge to the confined zone through SO_4 reduction processes and ^{34}S enrichment. Line B reflects mixing of the SO_4-depleted groundwater in the confined zone (Group III-B) with SO_4-rich ground water with a high $\delta^{34}S_{SO_4}$ value, particularly along the eastern boundary of the aquifer (represented by Group III-C). M6 is groundwater from the underlying Jurassic aquifer and may represent a possible end-member for the saline groundwater in that aquifer. Line C represents mixing with SO_4-rich ground water with a high $\delta^{34}S_{SO_4}$ value in the southern Arava Valley.

and Fe contents (0.05–0.15 mM; Fig. 6), high $\delta^{18}O_{H_2O}$ (−5.6‰; $n = 1$) and d-excess (12.7‰), low $\delta^{34}S_{SO_4}$ (−13‰) and $\delta^{18}O_{SO_4}$ (+8‰), high $^{87}Sr/^{86}Sr$ (0.7079), high $\delta^{13}C_{DIC}$ (−4‰), and high ^{14}C (68 pmc) values.
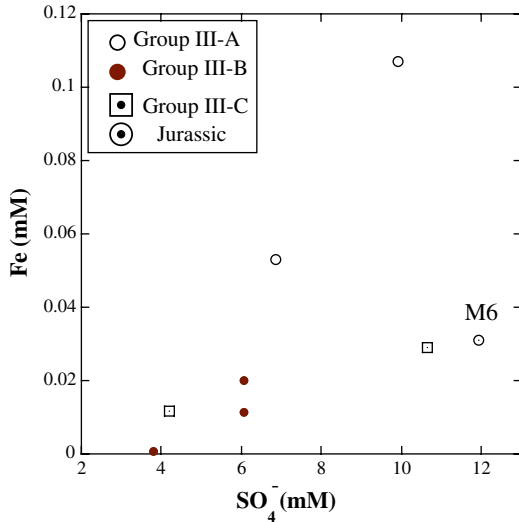

Fig. 6. Iron versus SO_4^{2-} contents (mmol/L) in groundwater from the northeastern Negev. Note the high Fe^{2+} and SO_4^{2-} contents in groundwater from the unconfined area relative to low concentrations in groundwater from the confined zone.
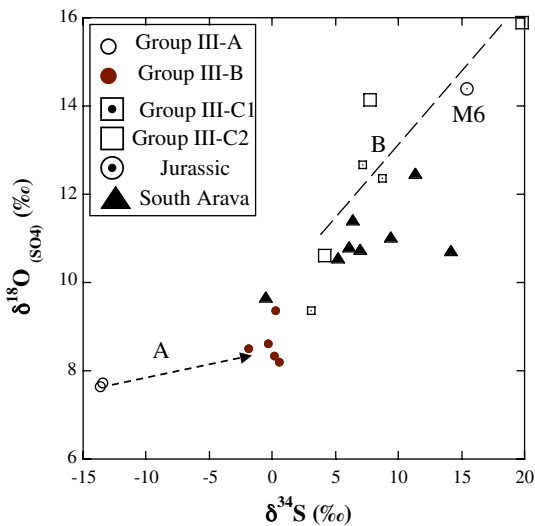
Fig. 7. $\delta^{18}O_{SO_4}$ versus $\delta^{34}S_{SO_4}$ values in groundwater from the NSA in the northeastern Negev (circles and squares) and Arava Valley (triangles). Arrow A reflects the possible evolution of groundwater from the unconfined to the confined zone through SO_4 reduction process. Line B reflects mixing of groundwater in both northeastern Negev (Group III-C) and southern Arava with groundwater sources characterized by high $\delta^{34}S_{SO_4}$ and $\delta^{18}O_{SO_4}$ values.

4.1.2. Group III-B

Deep groundwater that represents the confined zone (e.g., Yorqe'am 2A, Yorqe'am 4, and Makhtesh three wells; Fig. 2) and is characterized by relatively higher Cl concentrations (15.8–25.4 mM) and Br/Cl (0.9 to 1.3×10^{-3}), lower SO_4^{2-} content (3.4–6.8 mM), $\delta^{18}O_{H_2O}$ of $\sim-6.5 \pm 0.15$‰ ($n = 7$), relatively high d-excess (13.8–17.9‰; Fig. 4), higher $\delta^{34}S_{SO_4}$ (~-2‰) and $\delta^{18}O_{SO_4}$ ($\sim+8.5$‰; Fig. 7), lower $^{87}Sr/^{86}Sr$ (0.70774–0.70779), lower ^{14}C (0.2–2.3 pmc), and lower $\delta^{13}C_{DIC}$ values (−7.3 to −8.8‰) as compared to the unconfined zone (Group III-A).

4.1.3. Group III-C

Groundwater along the eastern boundary of the NSA that is adjacent to the Rift Valley faults (e.g., Ye'elim 3, Admon 2, and Admon 5 wells). The groundwater is saline with the highest Cl contents reported in this study (18.7–66.5 mM), high SO_4^{2-} (4.2–19.5 mM), marine Br/Cl ratio ($\sim1.5 \times 10^{-3}$), a wide range of $\delta^{18}O_{H_2O}$ (−7.6 to −6.7‰; $n = 5$), a wide range of d-excess (7.7–18‰), high $\delta^{34}S$ (up to +7‰) and $\delta^{18}O_{SO_4}$ (+14.1‰), and slightly low $^{87}Sr/^{86}Sr$ ratios
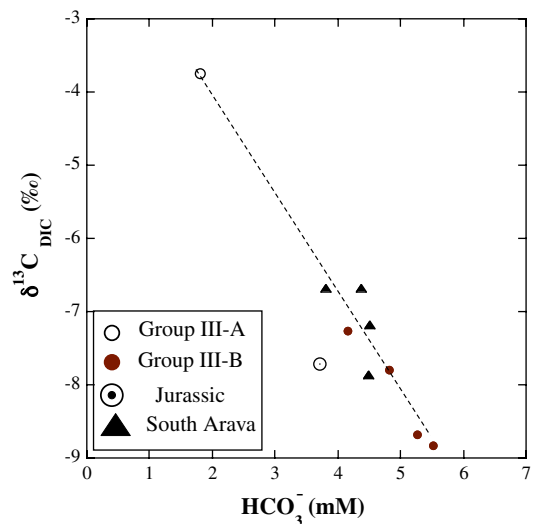

Fig. 8. $\delta^{13}C_{DIC}$ values versus HCO_3^- contents (mmol/L) in groundwater from the NSA in the northeastern Negev (circles) and Arava Valley (triangles and squares). The linear correlation between $\delta^{13}C_{DIC}$ and HCO_3^- suggests mixing between a HCO_3-rich source that is depleted in ^{13}C and recharge water with lower HCO_3^- and a higher $\delta^{13}C_{DIC}$ value. It is suggested that SO_4^{2-} reduction processes would generate high HCO_3^- with a depleted ^{13}C signature, while carbonate dissolution in the recharge zone would produce HCO_3^- with a relatively high $\delta^{13}C_{DIC}$ value.
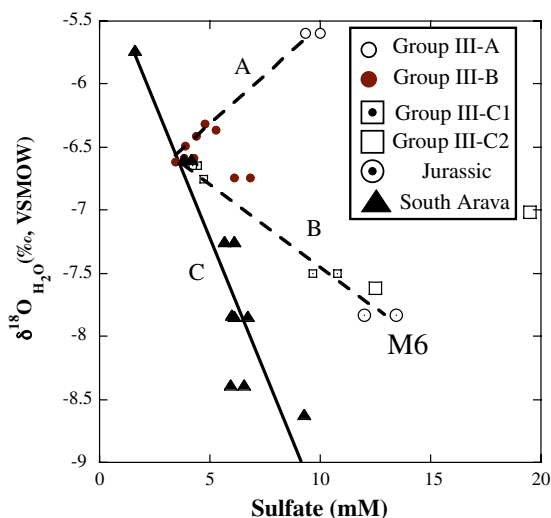
Fig. 9. $\delta^{18}O_{H_2O}$ values versus SO_4^{2-} contents (mmol/L) in groundwater from the NSA in the northeastern Negev (circles and squares) and Arava Valley (triangles). Line A represents possible evolution from the recharge to the confined zone through different recharge regimes. Line B reflects mixing of the SO_4-depleted groundwater in the confined zone (Group III-B) with SO_4-rich ground water with a low $\delta^{18}O_{H_2O}$ value, particularly along the eastern boundary of the aquifer (represented by Group III-C). M6 is groundwater from the underlying Jurassic aquifer and may represent a possible end-member for the saline groundwater in that aquifer. Line C represents mixing with SO_4^{2-}-rich ground water with a low $\delta^{18}O_{H_2O}$ value in the southern Arava Valley.
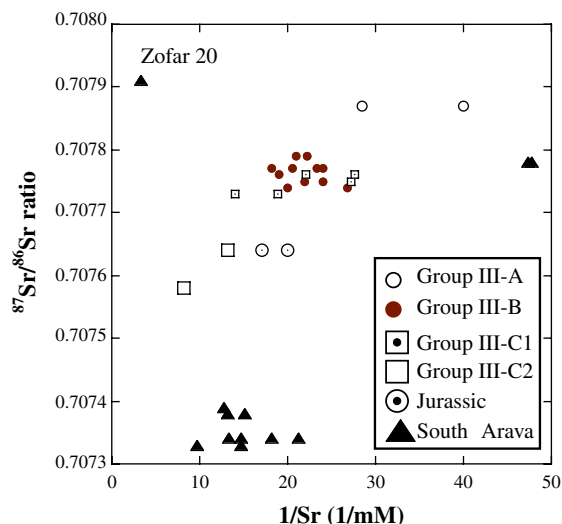

Fig. 10. Reciprocal of Sr content (l/mM) versus $^{87}Sr/^{86}Sr$ ratios in groundwater sampled from the NSA in the northeastern Negev (circles and squares) and Arava Valley (triangles). Groundwater samples from the Southern Arava have significantly lower $^{87}Sr/^{86}Sr$ ratios. In some cases (e,g., Zofar 20) the $^{87}Sr/^{86}Sr$ ratio of the groundwater from the southern Arava Valley is much higher, reflecting mixing with Rift Valley Ca-chloride brines rather than Paleozoic brines with low $^{87}Sr/^{86}Sr$ ratios. The linear correlation between 1/Sr and $^{87}Sr/^{86}Sr$ ratios in the northeastern Negev suggests mixing of Sr-rich groundwater derived from dissolution of Triassic gypsum ($^{87}Sr/^{86}Sr \sim 0.7076$) and recharge water with a higher $^{87}Sr/^{86}Sr$ ratio.

(0.7076 ± 0.0007; $n = 5$) as compared to Group III-B.

In addition, it was found that groundwater from the underlying Jurassic aquifer (represented by Makhtesh 6 well, referred to as "M6" in Figs. 5–11) is characterized as follows: Cl ~ 17 mM, $SO_4^{2-} \sim 13$ mM, Br/Cl $= 1.3 \times 10^{-3}$, $\delta^{18}O_{H_2O} = -7.8‰$, d-excess $= 12.1‰$, $\delta^{34}S_{SO_4} = +15‰$, $\delta^{18}O_{SO_4} = +14‰$ (Fig. 7), $^{87}Sr/^{86}Sr = 0.70764$, $^{14}C = 1.5$ pmc, and $\delta^{13}C$ values $= -7.7‰$.

4.2. Southern Arava Valley – flow regime I

Groundwater from the southern Arava Valley is characterized by relatively low Cl (2.3–21.4 mM) and SO_4^{2-} (1.6–6.4 mM) contents, relatively high Br/Cl (2.5×10^{-3}), predominantly low $\delta^{18}O_{H_2O}$ (five samples with $\delta^{18}O_{H_2O}$ ranging from $-8.7‰$ to $-7.25‰$ but with two heavier samples -6.6 and $-5.7‰$), low d-excess ($\sim 10‰$), a large range of $\delta^{34}S_{SO_4}$ (-0.5 to $+11.3‰$) and $\delta^{18}O_{SO_4}$ ($+9.7$ to $+12.5‰$), conspicuously low $^{87}Sr/^{86}Sr$ ratios

(0.70735), low ^{14}C (0.6–5.7 pmc), and $\delta^{13}C$ values (-7.3 to $-8.8‰$). The only exception from these values is the Zofar 20 well with exceptionally high salinity (Cl ~ 100 mM) and significantly different chemical and isotopic compositions (Table 1).

5. Discussion

5.1. The origin of groundwater: Sinai versus local recharge

According to the conventional interpretation (e.g., Issar et al., 1972; Issar, 1981; Rosenthal et al., 1998), groundwater in the NSA in the Negev and Arava Valley in Israel is exclusively derived from subsurface flow of groundwater from the Sinai Peninsula with a characteristic d-excess (deuterium excess) value of $\sim 10‰$. Indeed, most of the groundwater from the Arava Valley as well as the SO_4-rich groundwater from the northeastern Negev (Group III-C) and underlying Jurassic aquifer (M6) have d-excess values similar to those in groundwater from Sinai, possibly suggesting a common origin.
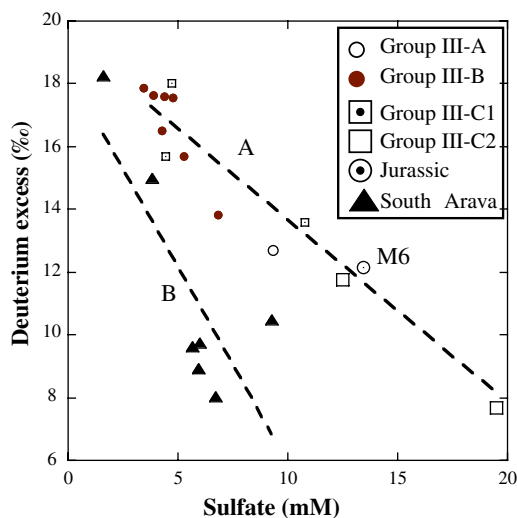
Fig. 11. Deuterium excess values versus SO_4^{2-} contents (mmol/L) in groundwater samples from the NSA in the northeastern Negev (circles and squares) and Arava Valley (triangles). Note the relatively lower d-excess values in the southern Arava relative to the confined zone in the northeastern Negev (Group III-B). Line A reflects mixing with a high-SO₄ source characterized by a low d-excess value particularly in the eastern part of the northeastern Negev. Line B reflects similar mixing in the southern Arava Valley.

In contrast, Fig. 4 shows that the low-SO₄ groundwater from the confined area in the northeastern Negev (Group III-B) has relatively high $\delta^{18}O_{H_2O}$ and δ^2H values and high d-excess values of ∼16‰, pointing towards a different origin and/or evolution of this groundwater.

Many studies have attempted to use differences in d-excess values to determine the time of groundwater recharge under different climatic conditions (see Clark and Fritz, 1997). Several processes, such as evaporation during or after rain infiltration, can influence the d-excess value of the residual groundwater. An important criterion for identifying the meteoric origin of groundwater relative to post-precipitation processes is the relationship between $\delta^{18}O_{H_2O}$ and δ^2H values. Groundwater with a $\delta^2H/\delta^{18}O_{H_2O}$ slope of ∼8 indicates origin from meteoric water with minimal post-precipitation effects, whereas a slope <8 may reflect evaporation during or after rainfall and/or mixing with an external water source with high $\delta^{18}O_{H_2O}$ and δ^2H values. The data (Fig. 4) show that groundwater from the confined area (Group III-B) has a $\delta^2H/\delta^{18}O_{H_2O}$ slope of ∼8 and thus the d-excess value is an indicator for the nature of the meteoric water during the aquifer replenishment, reflecting the relative humid-

ity in the atmosphere during the formation of the vapor (Gat, 1981, 1983). Groundwater with different d-excess values was probably formed under different climatic conditions or at least from different moisture sources. Since the NSA is a continuous basin from Sinai Peninsula to the in northeastern Negev (Fig. 1), one would expect that the isotopic imprints of O and H in the upstream groundwater in the aquifer would have prevailed in downstream groundwater. The different d-excess values thus implies that the origin of groundwater in the confined area of the NSA in northeastern Negev (d-excess ∼ 16‰) may be different than groundwater from the Arava Valley and the Sinai Peninsula (also with a $\delta^2H/\delta^{18}O_{H_2O}$ slope of ∼8 and d-excess ∼10‰), thus questioning the hypothesis that all groundwater in the NSA has a common origin in the Sinai Peninsula.

It has been suggested that low d-excess values around 10‰ indicate palaeo-recharge (>30 ka PB), while higher d-excess values (>20‰) indicate modern-day recharge to the NSA (Gat and Galai, 1982; Yechieli et al., 1992). Indeed, Levin et al. (1980) showed that modern precipitation over the Negev is characterized by d-excess values in the range of 15–25‰ which falls between the d-excess values of the Global Meteoric Water Line (∼10‰) indicative of more humid climates, and those of modern arid Mediterranean air masses (∼22‰; Gat and Carmi, 1970; Gat, 1981). Therefore, one could argue that the high d-excess values found in the confined zone in the northeastern Negev (Group III-B) are modern, particularly since modern groundwater from the overlying Avedat aquitard with modern-day ³H levels (Levin et al., 1980) has similarly high d-excess values of 15–20‰. However, the $\delta^{18}O_{H_2O}$ and δ^2H values in the NSA are significantly lower than those of the Avedat aquitard. In addition, the groundwater from the NSA in the Negev contains no ³H (Yechieli et al., 1992), and ¹⁴C activities are very low (see below), suggesting a different recharge regime for groundwater from the NSA in the northeastern Negev. The combined isotope evidence strongly suggests that groundwater from the confined section of the NSA in northeastern Negev is different from modern groundwater in the area and clearly has a different origin than groundwater from the southern Arava and the Sinai Peninsula. The most probable source for this groundwater is from local recharge in areas where the NSA is not confined along the major anticlines ("makhteshim") of the northeastern Negev.

In contrast, groundwater from the southern Arava has very similar isotope values to groundwater from the Sinai Peninsula with low $\delta^{18}O_{H_2O}$, δ^2H, and a similar d-excess value ($\sim10‰$). These values reflect groundwater replenishment under more humid climatic conditions during earlier times (Gat and Issar, 1974; Yechieli et al., 1992; Gat and Magaritz, 1980; Gat and Galai, 1982; Abed El Samie and Sadek, 2001). In fact, most of the palaeo-groundwater (i.e., ^{14}C ages >30 ka BP) along the Sahara and Western Desert in Egypt have d-excess values of $\sim10‰$ or even lower (Sonntag et al., 1978; Sultan et al., 1997). This suggests, that the confined groundwater in the southern Arava originated from lateral flow from the Sinai Peninsula (Gat and Issar, 1974).

The differences in the d-excess values in the three water groups in the northeastern Negev suggest multiple recharge phases in the region: (1) modern local recharge ($^{14}C = 67$ pmc; see later in this paper and Yechieli et al., 1997) under modern arid conditions yielding the highest $\delta^{18}O_{H_2O}$ and δ^2H values (Group III-A; unconfined aquifer of NE Negev); (2) past local recharge from a source with d-excess $\sim16‰$ and relatively lower $\delta^{18}O_{H_2O}$ and δ^2H values (Group III-B; confined aquifer of NE Negev); and (3) past recharge from a source with d-excess $\sim10‰$ with the lowest $\delta^{18}O_{H_2O}$ and δ^2H values (Group III-C), indicating either subsurface flow of depleted ^{18}O and ^2H groundwater from the Sinai Peninsula or local recharge in the northeastern Negev with a distinguished low d-excess value. If the latter is the case, it means progressively increasing aridity over the northeastern Negev with continuous rise of the d-excess values of the recharged water. The possible timing of the different recharge events will be discussed in Section 5.3.

It is concluded that the replenishment of the NSA and underlying Jurassic aquifer did not occur from a single source in Sinai Peninsula as previous models suggested (e.g., Issar et al., 1972; Issar, 1981; Rosenthal et al., 1998) but rather from multiple air masses with different isotopic characteristics and recharge zones in the Negev.

5.2. The origin of the solutes: Sources of sulfate-rich groundwaters

5.2.1. Sulfide oxidation and bacterial sulfate reduction

Previous studies have attributed the enrichment of SO_4^{2-} and the lack of a balance between Ca^{2+} and SO_4^{2-} in the NSA aquifer to dissolution of Ca- and Mg-sulfate salts and/or chemical fractionation in the unsaturated zone (Yechieli et al., 1992). The basic assumption of these studies was that recharge in arid zones may be associated with formation and recycling of sulfate salts in the recharge areas. The $\delta^{34}S_{SO_4}$ and $\delta^{18}O_{SO_4}$ data (Table 2) suggest an alternative explanation. The low $\delta^{34}S_{SO_4}$ and $\delta^{18}O_{SO_4}$ values of shallow groundwater in the unconfined area of the NSA in the northeastern Negev clearly indicate that the SO_4^{2-} is primarily derived from oxidation of pyrite. Recycling of meteoric S in the unsaturated zone via evaporation, gypsum precipitation and dissolution would preserve the meteoric S isotopic signature ($\delta^{34}S_{SO_4}$ range of $0‰$ to $+15‰$; Herut et al., 1995). In the northern Negev meteoric S is characterized by a $\delta^{34}S_{SO_4}$ value of $\sim+15‰$ (Issar et al., 1988), which is significantly higher than the value of $-13‰$ observed in groundwater SO_4^{2-} from the unconfined zone. In addition, the high Fe content that characterizes the SO_4-rich groundwater in the unconfined area of the NSA (Fig. 6) provides additional evidence for oxidation of pyrite under conditions that oxidation of disulfide proceeds at a lower redox potential than full Fe^{2+} oxidation.

Pyrite oxidation generates acidity, and thus the relatively high $^{87}Sr/^{86}Sr$ ratio (0.7079) that was observed in this groundwater may be attributed to dissolution of carbonate and/or silicate minerals with a higher $^{87}Sr/^{86}Sr$ ratio in the soil overlying the NSA. The low Br/Cl ratios that also characterize the shallow groundwater indicate halite dissolution. The high Na/Cl ratio (>1.1; Table 1) suggests further Na^+ release from water–rock interactions such as plagioclase dissolution or cation-exchange with clay minerals in the soil.

As discussed above, the water from the unconfined area (Group III-A) and from the confined area (Group III-B) formed during two distinct recharge phases. However, it is reasonable to assume that both water groups were subject to similar processes during their infiltration through the unconfined part of the aquifer. Therefore, the relatively low concentrations of SO_4^{2-} and the higher $\delta^{34}S_{SO_4}$ (Fig. 5) and $\delta^{18}O_{SO_4}$ values (Fig. 7) in the confined zone relative to the unconfined area are consistent with oxidation of the abundant organic matter in the aquifer matrix (mainly coal) associated with bacterial (dissimilatory) SO_4 reduction. It is important to note that the $\delta^{34}S$ and $\delta^{18}O_{SO_4}$ values of this groundwater deviate from a possible

mixing relationship between recharge water (Group III-A) and underlying Jurassic groundwater towards a lower $\delta^{34}S_{SO_4}/\delta^{18}O_{SO_4}$ slope (Fig. 7). Consequently, it is argued that the SO_4-rich shallow groundwater with low $\delta^{34}S_{SO_4}$ values from the recharge zone was modified into low-SO_4^{2-} and relatively high-$\delta^{34}S_{SO_4}$ ($\sim 2\permil$) groundwater in the confined zone via bacterial SO_4 reduction. This process results in formation of HCO_3^- and H_2S gas. Indeed, low-SO_4 groundwater from the confined zone is associated with relatively high HCO_3^- contents (Table 1). These variations are also consistent with the increase of $\delta^{34}S_{SO_4}$ and $\delta^{18}O_{SO_4}$ values (Fig. 7) and the decrease of $\delta^{13}C_{DIC}$ values (Fig. 8) caused by the contribution of organic C with low $\delta^{13}C$ values to HCO_3^-.

In addition to the isotopic variations, two independent lines of evidence support the hypothesis of bacterial SO_4 reduction in the confined zone of the NSA. The first is the high H_2S contents that have been reported for this groundwater by the local water company (Mekorot Ltd.; a range of 2.9–5.6 ppm in the wells of Makhtesh 3 and Makhtesh 4) relative to negligible amounts in the recharge zone (a range of 0–0.3 ppm in the wells of Makhtesh 1 and Makhtesh 5). The second line of evidence is the relatively low Fe content in groundwater from the confined area (Fig. 6). As H_2S is generated during bacterial SO_4 reduction, it is likely that it will rapidly react with dissolved Fe in the aquifer and form Fe sulfide minerals, thus decreasing the overall Fe content in the residual groundwater. In most of the groundwater from the NSA, dissolved Fe occurs in reduced form (Fe^{2+}), and during water production from the wells the anoxic groundwater containing Fe^{2+} is rapidly oxidized and Fe-oxides are precipitated.

Bacterial (dissimilatory) SO_4 reduction (BSR) is a process that causes decreasing SO_4^{2-} concentrations while enriching the remaining SO_4^{2-} in ^{34}S and ^{18}O (e.g. Harrison and Thode, 1957). In a closed system, isotope fractionation during BSR can be described by the Rayleigh equation:

$$R_t = R_0 f^{(\alpha-1)} \qquad (2)$$

where R_t and R_0 are the S isotope ratios of SO_4^{2-}, f is the ratio between SO_4^{2-} concentration at time t (C_t) and the initial concentration of SO_4^{2-} (C_0), and α is the isotopic fractionation factor. Using δ values, Eq. (2) can be re-written as follows:

$$\delta_t = (\delta_0 + 1000)f^{(\alpha-1)} - 1000 \qquad (3)$$

Assuming that the chemical composition of the water before bacterial SO_4 reduction was similar to that in the present-day unconfined water (i.e., $C_0 = 10$ mM and $\delta^{34}S_0 = -13\permil$) the isotopic fractionation factor that is required to lower the SO_4^{2-} concentration in the groundwater of the confined aquifer to the lowest measured value (i.e., $C_t = 3.65$ mM and $\delta^{34}S_t = 0.1\permil$) was calculated using Eq. (3) to be $\alpha = 1.013$. Isotope fractionation factors for S during bacterial (dissimilatory) SO_4 reduction can be quite variable, depending upon environmental conditions (Canfield, 2001), but typically range between 1.010 and 1.020 in hydrological settings (e.g., Strebel et al., 1990). This range is consistent with the fractionation factor determined above for the confined groundwater in the northeastern Negev (i.e., $\alpha = 1.013$).

5.2.2. Mixing with external sulfate-rich water sources
5.2.2.1. Northeastern Negev.
The third water source (Group III-C) in the northeastern Negev is saline SO_4-rich groundwater along the eastern margin of the NSA that is characterized by low $\delta^{18}O_{H_2O}$, low $^{87}Sr/^{86}Sr$, and high $\delta^{34}S_{SO_4}$ and $\delta^{18}O_{SO_4}$ values (Figs. 5, 7, 9 and 10). This water group may be subdivided into two sub-groups: C1 – the water from the Tamar wells (Fig. 1b), which are similar in their salinity to the other water of the confined aquifer (Group III-B); and C2 – water with significantly higher salinity from the northern wells of Yeelim and Admon (Fig. 1C). It is suggested that the water of group C1 is derived from mixing of groundwater from Group III-B with groundwater from the underlying Jurassic aquifer water (M6) having $^{87}Sr/^{86}Sr = 0.70764$ and a $\delta^{34}S$ value of $+15\permil$. This interpretation is based on linear correlations between SO_4^{2-} and $\delta^{34}S_{SO_4}$ (Fig. 5), SO_4^{2-} and $\delta^{18}O_{H_2O}$ (Fig. 9), and SO_4^{2-} and d-excess (Fig. 11), in which the composition of Jurassic aquifer water (M6) represents a possible end-member. Some of the more saline waters (sub-group C2) are located on the same mixing line, but given their high Cl^- and SO_4^{2-} contents it seems that their composition was also affected by another source of salinity.

The correlations between SO_4^{2-} concentrations and $\delta^{18}O_{H_2O}$ values (Fig. 9) and SO_4^{2-} and d-excess (Fig. 11) suggest that a significant fraction of the groundwater in the eastern part of the NSA in the northeastern Negev, particularly along the aquifer's eastern margin, is derived from mixing with SO_4-rich groundwater from the underlying Jurassic aquifer. Variations in the $\delta^{34}S_{SO_4}$, $\delta^{18}O_{SO_4}$ values and

SO_4^{2-} concentrations were used to calculate the relative contribution of the external SO_4-rich source, and found that it can contribute up to 80% of the salts dissolved in groundwater from the NSA in the northeastern Negev. The extent of contribution from the SO_4-rich source was found to vary locally. For example, while the water from the Tamar 9 (Fig. 1b) well is geochemically similar to the other groundwater of the confined aquifer, the composition of the water from the adjacent Tamar 11 well is strongly influenced by water from the Jurassic aquifer. In conclusion, it is suggested that the combined evidence from Sr and S isotope ratios indicates a significant flow of groundwater from the underlying Jurassic aquifer into the eastern part of the NSA.

Given the $\delta^{34}S_{SO_4}$ and $^{87}Sr/^{86}Sr$ variations in the NSA and the Jurassic aquifer in the northeastern Negev, it is suggested that the SO_4^{2-} source of the high SO_4-containing groundwater is dissolution of the underlying massive marine Triassic anhydrite deposit (Mohila Formation; Druckman, 1974). Secular variations of $^{87}Sr/^{86}Sr$ and $\delta^{34}S_{SO_4}$ values in seawater through time are recorded in marine sulfates since both S and Sr isotopes undergo at most minor isotope fractionation during gypsum precipitation from seawater. Likewise, dissolution of sulfate minerals by groundwater would not modify the original $^{87}Sr/^{86}Sr$ and $\delta^{34}S$ signatures. During the late Triassic, seawater had an $^{87}Sr/^{86}Sr$ signature of ~0.7076 (Burke et al., 1982; Korte et al., 2003; Veizer, 1989; Veizer and Compston, 1974; Veizer et al., 1997, 1999) and a $\delta^{34}S_{SO_4}$ range of +8‰ to +15‰ (Kampschulte and Strauss, 2004). Nissenbaum (1978) reported a $\delta^{34}S_{SO_4}$ range of +15.7‰ to +16.6‰ in gypsum from Middle to Upper Triassic from the northern Negev that is consistent with the groundwater isotopic results of >+15‰.

The relatively high salinity of the groundwater from the Northern Arava Valley (Yeelim and Admon wells) along the eastern boundary of the NSA (Sub-group C2; Fig. 4) indicates that either some of the underlying groundwater from the Jurassic aquifer is also saline or that there is another source of salinity. The first possibility is consistent with Nativ (1987) who reported brackish groundwater in the Jurassic aquifers in the northeastern Negev. Given that the most saline groundwater has a Br/Cl ratio (1.4×10^{-3}) that is similar to that of seawater, any contribution of hypersaline brine from the Rift valley that typically have higher Br/Cl ratios (Yechieli et al., 1992; Guttman et al.,

1999) is ruled out. Instead, the approach of Issar (1981) is followed, suggesting that the salinity may be derived from remnants of seawater that was not effectively flushed from the aquifer. Hence, the composition of the saline groundwater from the eastern part of the NSA may indicate a mixture of three components; diluted connate seawater, groundwater from the underlying Jurassic aquifer that is influenced by dissolution of anhydrite with low $^{87}Sr/^{86}Sr$ and high $\delta^{34}S$ values, and fresh water with d-excess ~10‰.

5.2.2.2. Southern Arava. In the southern Arava valley the positive relationships between Cl^- and Br^- (Fig. 3) and between SO_4^{2-} and $\delta^{34}S_{SO_4}$ values (Fig. 5) indicate that the groundwater is derived from a source with high $\delta^{34}S_{SO_4}$ and Br/Cl values. However, the $^{87}Sr/^{86}Sr$ values measured in the groundwater (0.70735) are lower than the Triassic oceanic signature (0.7076; Burke et al., 1982; Korte et al., 2003; Veizer, 1989; Veizer and Compston, 1974; Veizer et al., 1997, 1999). In addition, due to the major unconformity of the Negev, the Jurassic aquifer units do not exist in the southern Negev and Arava valley (Nativ, 1987; Nativ et al., 1987). Thus, the SO_4-rich groundwater cannot be derived from dissolution of Triassic anhydrite as suggested for the northeastern Negev, but rather from another source with a significantly lower $^{87}Sr/^{86}Sr$ ratio.ource with a significantly lower $^{87}Sr/^{86}Sr$ ratio.

Conspicuously low $^{87}Sr/^{86}Sr$ ratios (0.7061) were reported in SO_4-rich saline water (TDS up to 13 g/L) in the vicinity of Timna in the southern Arava valley (Beyth et al., 1981). The saline water from Timna is characterized by high Br/Cl ratios (~3×10^{-3}; Fig. 4) and has a Ca-chloride composition (i.e., $Ca/(SO_4 + HCO_3) > 1$). In addition, the saline water from Timna has a low $\delta^{18}O_{H_2O}$ value (−9‰; Rosenthal et al., 1992). These geochemical and isotopic signatures are similar to those of groundwater from the NSA in the southern Arava Valley, although the $\delta^{34}S_{SO_4}$ value of Timna brines is not known. Given the Ca-chloride composition and the high Br/Cl ratio, Beyth et al. (1981) suggested that the saline water from the Timna is a remnant of the Rift-Valley brine that interacted with mafic/basaltic rocks with a low $^{87}Sr/^{86}Sr$ ratio. Gavrieli et al. (2001) showed that Ca-chloride brines from the Rift Valley typically have high $\delta^{34}S_{SO_4}$ (>20‰) values due to bacterial SO_4 reduction. Consequently, the good correlations between SO_4^{2-} concentrations and $\delta^{34}S_{SO_4}$ values (Fig. 5) and SO_4^{2-}

concentrations and $\delta^{18}O_{H_2O}$ values (Fig. 9) suggest a single source for both the groundwater from the NSA and Timna waters. The lack of any hydrological barrier between the NSA and the Paleozoic units in the southern Negev (Nativ et al., 1987) makes it feasible that groundwater from the NSA is mixed with underlying brines from the Paleozoic aquifer.

Previous studies suggested that the groundwater composition in the southern Arava Valley is derived from a mixture of two flow regimes: (1) a western flow component derived from Sinai and the southern Negev with distinctively low $\delta^{18}O_{H_2O}$ values; and (2) eastern flow from recharge in Edom Mountains in Jordan with higher $\delta^{18}O_{H_2O}$ values (Rosenthal et al., 1990; Adar et al., 1992; Guttman et al., 1999). The positive linear correlations between SO_4^{2-} concentrations and $\delta^{34}S_{SO_4}$ values and SO_4^{2-} concentrations and $\delta^{18}O_{H_2O}$ values (Figs. 5 and 9) indicate that the western component has high SO_4^{2-} content and $\delta^{34}S_{SO_4}$ values. Indeed, groundwater from Shizafon 1 well (Fig. 1), which is the most western sampling point in the southern Arava Valley, has the highest SO_4^{2-} concentration and $\delta^{34}S_{SO_4}$ value. If the high SO_4^{2-} groundwater indeed originated in the Sinai Peninsula, one would expect it to have low $\delta^{34}S_{SO_4}$ values and high $^{87}Sr/^{86}Sr$ ratios consistent with the observations for groundwater recharged in the northeastern Negev. Alternately, if bacterial SO_4 reduction in the confined zone modified the recharged water, one would expect to find low SO_4^{2-} contents associated with high $\delta^{34}S_{SO_4}$ values. In contrast, the authors found that the western groundwater flow component had high SO_4^{2-} concentrations, high $\delta^{34}S_{SO_4}$ values, and low $^{87}Sr/^{86}Sr$ ratios similar to the composition observed in the Timna brines (Beyth et al., 1981). This may suggest that a significant fraction of the western groundwater flow component is derived from mixing with Timna brines, and is hence not derived entirely from the previously suggested recharge water in southern Sinai.

The most saline groundwater (Zofar 20 well) found in the southern Arava is characterized by relatively low SO_4^{2-} content (Table 1), high Br/Cl ($\sim 4 \times 10^{-3}$; Fig. 3), and high $^{87}Sr/^{86}Sr$ ratios (0.70791; Fig. 10) clearly reflecting an intrusion of a typical Rift Valley brine with a Ca-chloride composition (Yechieli et al., 1992; Guttman et al., 1999). The $^{87}Sr/^{86}Sr$ ratio is therefore a useful tool to delineate different sources of salinity and to discriminate between upconing of Neogene Rift Valley brines

(high $^{87}Sr/^{86}Sr$) and mixing with brines from the Paleozoic aquifer (low $^{87}Sr/^{86}Sr$).

It should be noted that in many aquifers in sedimentary rocks, the groundwater Sr isotopic composition is determined by dissolution of the aquifer matrix (e.g., Harrington and Herczeg, 2003) and/or ion-exchange with clay minerals in the aquifers (e.g., Johnson and DePaolo, 1994; Armstrong et al., 1998). Carbonate and sulfate minerals contain Sr^{2+} in their crystalline lattice with $^{87}Sr/^{86}Sr$ ratios identical to the original solution from which these minerals were precipitated. The $^{87}Sr/^{86}Sr$ ratios of silicate minerals, however, depends on their Rb^+ content, age, and initial fluid composition (Harrington and Herczeg, 2003). In a case of weathering of Precambrian granitic rock as in the NSA, one would expect that weathering of silicate minerals would result in formation of groundwater with high $^{87}Sr/^{86}Sr$ ratios. Indeed, saline groundwater from a similar (Kurnub Group) aquifer in central Jordan yields a high $^{87}Sr/^{86}Sr$ ratio (Zarqa River; $^{87}Sr/^{86}Sr$ ~ 0.7087; Farber et al., 2004). Likewise, the $^{87}Sr/^{86}Sr$ ratios of groundwater from the sandstone Disi aquifer in southern Jordan are in the range of 0.7083–0.7116 (Vengosh and Bullen, unpublished data).

In contrast, most of the groundwater from the Negev and Arava Valley is characterized by a positive correlation between SO_4^{2-} concentration and $\delta^{34}S$ values (Fig. 5) and an inverse correlation between Sr^{2+} and $^{87}Sr/^{86}Sr$ (Fig. 10), implying mixing with an end-member characterized by high SO_4^{2-} concentrations and a low $^{87}Sr/^{86}Sr$ ratio (<0.7080). In the northeastern Negev it is suggested that groundwater from the NSA is mixed with groundwater from the underlying Jurassic aquifer whereas in the southern Arava Valley it is suggested that the groundwater is mixed with brines from the underlying Paleozoic aquifers. In both areas, the idea of a contribution of groundwater from underlying aquifers is new and requires a major change in the previous hydrogeological concepts that considered only lateral flow within the NSA from presumed recharge from outcrops in the southern Sinai Peninsula.

5.3. The age of the groundwater: the impact of bacterial sulfate reduction

The ^{14}C activity of the recharge water (Makhtesh 1 well) is high (67 pmc) and indicates that the water is modern or relatively young (residence time $\leqslant 3200$ a). Yechieli et al. (1997) reported similar

results (^{14}C range of 50–70 pmc) for young (^{3}H-containing) groundwater in shallow aquifers in the Arava Valley. The relatively high δ^{13}C value of DIC of $-3.8\permil$ suggests that the original ^{14}C composition may have been affected by dissolution of ^{14}C-free carbonate minerals, which is consistent with the high ^{87}Sr/^{86}Sr ratios that characterize the water from the unconfined area. In contrast, ^{14}C activity values of groundwater in the confined zone in the northeastern Negev (Group III-B) are significantly lower, ranging from 0.2 to 2.3 pmc. Likewise, groundwater samples from the southern Arava Valley have low radiocarbon activity values between 0.6 and 5.8 pmc. Groundwater from the underlying Jurassic aquifer has also a low ^{14}C activity of 1.5 pmc. Using the end-member assumption that the activity of ^{14}C is solely determined by radioactive decay, the residence time of the water in the confined aquifer is significantly higher than that in the unconfined area and is in the range of 24–51 ka. However, as shown above, there is evidence that the groundwater in the confined aquifer acquired a significant amount of "dead" carbon via HCO_3^- formation during bacterial SO_4^{2-} reduction, which implies that the above stated groundwater mean residence times may be grossly overestimated and can only be considered a maximum age-limit. In the following discussion, the authors try to estimate the minimum residence times of the groundwater.

In spite of the differences in the $\delta^{18}O_{H_2O}$, δ^2H, and d-excess values, groundwater samples from both the northeastern Negev and Arava Valley have similarly low ^{14}C values. In addition, $\delta^{13}C_{DIC}$ values in the confined aquifers of northeastern Negev and Arava Valley are significantly lower than in the recharge area, indicating that from a mass-balance perspective, decay alone cannot account for the decrease in ^{14}C activities. The overall negative correlation between HCO_3^- concentrations and $\delta^{13}C_{DIC}$ values (Fig. 8) indicates that there must be an additional source of C with a negative δ^{13}C value. Since carbonate dissolution would add C with δ^{13}C $\sim 0\permil$, the most likely source for the negative δ^{13}C values is the oxidation of organic matter from aquifer host rocks (δ^{13}C $\sim -25\permil$). Sulfate is the most common electron acceptor for oxidizing organic C.

As discussed earlier, bacterial SO_4 reduction removes SO_4^{2-}, according to the following generalized equation:

$$2CH_2O + SO_4^{2-} \rightarrow H_2S + 2HCO_3^- \qquad (4)$$
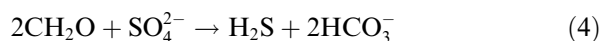
According to Eq. (4), the amount of dissolved inorganic C (DIC) that is generated in this process should be equivalent to the SO_4^{2-} loss (i.e., generation of two moles of HCO_3 per consumed mole of SO_4). This is clearly not the case in the studied aquifer. For example, if the original recharge water in the NSA had a composition similar to that of groundwater in the present day unconfined area of the aquifer (in Makhtesh 1 well, $SO_4^{2-} \sim 8$ mM; δ^{34}S $= -13\permil$) and it was modified due to bacterial SO_4 reduction to the composition in the deep and confined area (e.g., the deepest wells of En Yorqe'am 2 and En Yorqe'am 4; $SO_4^{2-} \sim 3.8$ mM; $\delta^{34}S_{SO_4} = +0.2\permil$; Fig. 5), the amount of loss SO_4^{2-} can be estimated to be about ~ 4 mM. The increase in HCO_3^- concentrations accounts for only ~ 3 mM (Fig. 8) out of ~ 8 mM expected HCO_3^- increase, and thus does not balance the apparent SO_4^{2-} loss. The relatively small increase in HCO_3^- is, however, not surprising. Considering that the groundwater in the recharge area is saturated with respect to calcite (Table 1), any further liberation of HCO_3^- from bacterial SO_4 reduction will inevitably result in an oversaturation of the groundwater and, therefore, in the precipitation of carbonate minerals. Both, the liberation of C by bacterial SO_4 reduction and the subsequent precipitation of carbonate must be taken into account when calculating ^{14}C ages based on C mass balance calculations.

In the southern Arava Valley the groundwater shows no evidence of bacterial SO_4 reduction and the positive correlation between SO_4^{2-} concentrations and $\delta^{34}S_{SO_4}$ values indicates mixing between high and low SO_4^{2-} groundwaters (Figs. 5 and 7). Nonetheless, the inverse relationship between the DIC concentrations and δ^{13}C values is identical to that of groundwater in the northeastern Negev (Fig. 8). Hence it is suggested that the original recharge water was also modified via bacterial SO_4 reduction, but mixing with an external water source with a high SO_4^{2-} (and low DIC) concentration has modified the original S isotopic composition of SO_4^{2-}.

Groundwater residence times were calculated using the geochemical code NETPATH 2.0 (Plummer et al., 1994) and taking bacterial SO_4 reduction and carbonate precipitation into account. For the calculations, several assumptions were made: (1) groundwater in the confined and deeper parts of the aquifers evolved from water with a chemical and isotopic signature similar to that found in the recharge areas (δ^{13}C $= -3.7\permil$; ^{14}C $= 67.7$ pmc);

(2) no further significant carbonate dissolution occurs in the saturated zone since groundwater is typically over-saturated with respect to calcite (7 out of 11 samples from the confined zone have Saturation Index (SI) values above zero); (3) assuming closed system conditions, the only additional source for DIC is via organic matter oxidation during bacterial SO_4 reduction in the aquifer; (4) HCO_3^- formed during bacterial SO_4 reduction is assumed to have $\delta^{13}C$ values of $-25\permil$ and contains no radio-carbon ($^{14}C = 0$ pmc); and (5) in the models, the processes of bacterial SO_4 reduction, HCO_3^- liberation and carbonate precipitation are constrained by $\delta^{13}C$ groundwater values.

Table 3 summarizes the results of the calculated groundwater mean residence times. The new estimates indicate that groundwater recharge occurred during the later stages of the Pleistocene between 14 and 38 ka BP. These estimates are up to 13 ka younger than estimates based on radioactive decay alone, clearly demonstrating that groundwater residence times can be grossly overestimated if aquifer processes such as water–rock interaction and/or bacterial SO_4 reduction are not taken into account. Due to the uncertainty in the amount of dead C that was added to the groundwater since recharge, it is not possible to obtain unambiguous ages based on the ^{14}C data. The two sets of residence time calculations presented in Table 3 were calculated using two differ-

ent sets of assumptions regarding the contribution of dead C to the activity of ^{14}C. It is suggested that the actual age of the water is bracketed by these two sets of calculations and is not older than 50 ka and not younger than 14 ka. Therefore, the calculations indicate that the groundwater in the confined aquifer is too old to be related to the present day recharge, but rather recharged during the Last Glacial Period.

6. Synthesis: regional implications

The O and H isotope data obtained in this study suggest that the Nubian sandstone aquifers and the underlying Jurassic aquifer in the Negev experienced several recharge events during the Pleistocene and Holocene. A comparison with the stable isotope data from the NSA in the Sinai Peninsula (Abed El Samie and Sadek, 2001) and Disi-Muawwara (Paleozoic sandstone) aquifer in southern Jordan (Bajjali and Abu-Jaber, 2001) shows (Fig. 12) that the isotopic composition of groundwater from the southern Arava Valley is similar to that of Sinai with relatively low $\delta^{18}O_{H_2O}$ and δ^2H values and d-excess $\sim10\permil$. In contrast, the relatively higher $\delta^{18}O_{H_2O}$ and δ^2H values measured in groundwater from the northeastern Negev partly overlap with those of the Disi aquifer (also with a $\delta^2H/\delta^{18}O_{H_2O}$ slope ~8), although the d-excess values in the Negev are slightly higher ($16\permil$ and $12\permil$, respectively;

Table 3
^{14}C and $\delta^{13}C$ compositions of groundwater from the Nubian Sandstone aquifer

Sample	Temperature	pH	$\delta^{13}C$ (‰)	^{14}C (pmc)	Age' (decay only)	Age' (modelled)
Northeastern Negev						
Unconfined Aquifer						
Ni-2	Makhtesh 1	28.1	7.2	−3.8	67.7	3230	Modern
Confined Aquifer						
Ni-8	Makhtesh 3	37	7.4	−8.8	1.2	36,844	22,632
Ni-4	Makhtesh 4	37.9	8.3	−7.8	2.3	31,043	21,217
Ni-6	Yorqe'am 1	34.2	8.7	−7.3	0.4	46,070	34,046
Ni-5	Yorqe'am 2A	37.1	8.1	−8.7	0.2	50,588	37,684
Jurassic Aquifer						
Ni-3	*Makhtesh 6*	*35.8*	*7.1*	*−7.7*	*1.5*	*34,830*	*12405 (?)*
Southern Arava						
Ni-17	Ye'elon 6A	38.8	9.3	−7.2	3.0	29,100	14,145
Ni-21	Grofit 4	31.3	8.9	−6.7	0.6	42,157	34,139
Ni-18	Ktora 5	33.4	5.9	−7.9	5.8	23,582	4351
Ni-20	Ye'elon 3A	34.3	8.5	−6.7	1.0	37,989	30,223

Groundwater residence time calculations of the ^{14}C data were carried out using the geochemical code Netpath 2.0 (Plummer et al., 1994), assuming only decay of ^{14}C and taking SO_4 reduction and carbonate precipitation into account (see text for details).
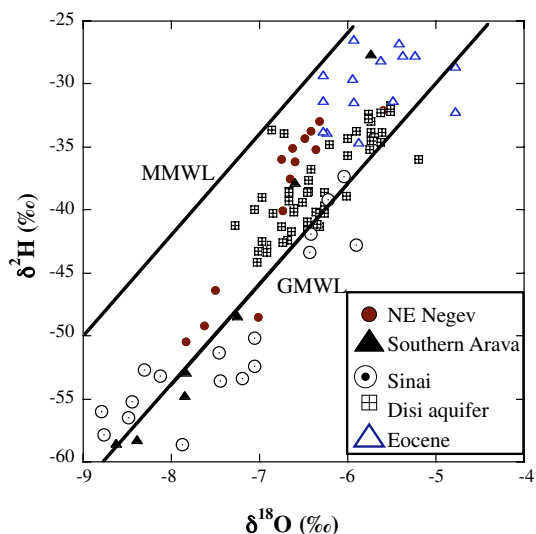
Fig. 12. δ^2H versus $\delta^{18}O_{H_2O}$ values of groundwater from the NSA in the northeastern Negev, Arava Valley, Sinai Peninsula (data from Abed El Samie and Sadek, 2001), Disi aquifer in southern Jordan (Bajjali and Abu-Jaber, 2001), and Avedat (Ecocene) aquifer in the Negev (Levin et al., 1980). Note the overlaps of the isotopic compositions in the northeastern Negev and Disi aquifer in Jordan, as well as the southern Arava Valley and Sinai Peninsula.

Fig. 12). This isotopic distinction suggests different recharge sources; a northern air mass with a high d-excess value that affected the northeastern Negev and southern Jordan (Fig. 1) and a southern air mass that was the source for the recharge water in the outcrops of the NSA in southern Sinai Peninsula. It is proposed that the northern air mass with a high d-excess value was derived from the Mediterranean (Gat, 1983), whereas the southern air mass with a d-excess value similar to that of the global meteoric water line represents recharge under higher humidity conditions.

Based on the similarity of the ^{14}C activities in groundwater from the northeastern Negev and in southern Arava Valley, one might suggest simultaneous recharge events in southern Sinai and northeastern Negev (and perhaps also in southern Jordan). However, given the uncertainties regarding the contribution of ^{14}C-free carbon by oxidation of organic C, carbonate dissolution, and mixing with underlying saline water in the southern Arava Valley, this hypothesis should be considered with caution. The low $\delta^{18}O_{H_2O}$, δ^2H and d-excess ($\sim 10‰$) values of both the saline groundwater from NSA in the northeastern Negev (Group III-C) and from the underlying Jurassic aquifer reveal that

recharge from a humid air mass also occurred in the Northeastern Negev. It is suggested that the recharge to the Jurassic aquifer is also local (and not derived from subsurface flow from Sinai Peninsula) given the relatively low salinity measured in Makhtesh 6 well as compared to the other saline groundwater samples of Group III-C (Fig. 3) and the high salinity reported for groundwater in the northern Sinai Peninsula (Abed El Samie and Sadek, 2001). Here again, the ^{14}C activity (1.5 pmc) of the Jurassic groundwater is not distinguishable from those of the overlying NSA. It is important to emphasize that the attempt to relate the ^{14}C-based residence times to recharge events is problematic because of potential groundwater mixing processes that at present cannot be fully taken into account because of the similarity of ^{14}C values in the various aquifer units. Therefore, one cannot exclude the possibility that groundwater in the southern Arava represents a mixture of very old groundwater ($\gg 50$ ka) as demonstrated in the western desert in Egypt (Sturchio et al., 2004; Patterson et al., 2005) and a younger water component with a detectable ^{14}C activity.

Recently it has been shown that gypsic-saline Reg soil profiles on flat alluvial surfaces in the southern Negev lack any evidence of mineral precipitation (i.e., no calcic horizons) since the middle Pleistocene and therefore it was suggested that the southern Negev has been permanently hyperarid during this period while wetter episodes occurred only in the northern Negev (Amit et al., 2006). Given that calcic soils in this region are an indicator for rainfall amount (>80 mm a^{-1}), it seems that hyperarid conditions (precipitation <50 mm a^{-1}) existed in the southern Negev during the last 200 ka (Amit et al., 2006). In addition, Ayalon et al. (1998) and Bar-Matthews et al. (2003) reported inverse relationships between the amount of rain and its $\delta^{18}O$ values in modern precipitation over central Israel, and argued that the ^{18}O-enriched isotopic composition measured in speleothems during the glacial period reflects arid conditions. According to the $\delta^{18}O$ data measured in speleothems from two caves in Israel, the last wet period occurred after the last glacial maximum, associated with the last sapropel S1 event in the eastern Mediterranean (10–8 ka BP). These results imply that major recharge to the NSA could have occurred during the Late Pleistocene in the northern Negev but no significant recharge had occurred in the southern Negev and perhaps also in Sinai Peninsula

during this period. If this is the case, the major recharge to the NSA is a much older event than previously anticipated as suggested for groundwater from the NSA in Egypt (e.g., Sturchio et al., 2004; Patterson et al., 2005). The ^{14}C data from groundwater in the southern Arava Valley cannot confirm this given the evidence for mixing with external saline groundwater with unknown ^{14}C activity.

In conclusion, it is argued that the traditional link (see in Clark and Fritz, 1997) between d-excess and ^{14}C tracers as proxies for groundwater-age determination in the NSA is not sufficient, given that relatively high d-excess values do not necessarily indicate modern groundwater. This study shows that an integration of a large spectrum of geochemical and isotopic tracers is essential in order to reconstruct the sources and the geochemical evolution of groundwater. Moreover, bacterial SO_4^{2-} reduction has crucial implications for the determination of groundwater ages and corrections for the contribution of ^{14}C free ('dead') carbon that are required in aquifers where bacterial SO_4 reduction has occurred. Groundwater ages estimated from ^{14}C activities should therefore always be interpreted very cautiously and a wide suite of geochemical and isotopic data should be consulted to correct measured ^{14}C activities for both geochemical processes in the aquifer (e.g., water rock interaction and bacterial SO_4 reduction) and mixing with external fluids having different ^{14}C activities.

Acknowledgements

References

Abed El Samie, S.G., Sadek, M.A., 2001. Groundwater recharge and flow in the Lower Cretaceous Nubian Sandstone aquifer in the Sinai Peninsula, using isotopic techniques and hydrochemistry. Hydrogeol. J. 9, 378–389.

Adar, E., Issar, A.S., Rosenthal, E., Batelaan, O., 1992. Quantitative assessment of flow pattern in the southern Arava Valley (Israel) by environmental tracers in a mixing cell model. J. Hydrol. 136, 333–354.

Amit, R., Enzel, Y., Sharon, D., 2006. Permanent Quaternary hyperaridity in the Negev, Israel, resulting from regional tectonics blocking Mediterranean frontal systems. Geology 34, 509–512.

Armstrong, S.C., Sturchio, N.C., Hendry, M.J., 1998. Strontium isotopic evidence on the chemical evolution of pore waters in the Milk River Aquifer, Alberta, Canada. Appl. Geochem. 13, 463–475.

Ayalon, A., Bar-Matthews, M., Sass, E., 1998. Rainfall–recharge relationships within a karstic terrain in the Eastern Mediterranean semi-arid region, Israel: δ^{18}O and δD characteristics. J. Hydrol. 207, 18–31.

Bajjali, W., Abu-Jaber, N., 2001. Climatological signals of the paleogroundwater in Jordan. J. Hydrol. 243, 133–147.

Bar-Matthews, M., Ayalon, A., Gilmour, M., Matthews, A., Hawkesworth, C., 2003. Sea–land oxygen isotopic relationships from planktonic foraminifera and speleothems in the Eastern Mediterranean region and their implication for paleorainfall during interglacial intervals. Geochim. Cosmochim. Acta 67, 3181–3199.

Beyth, M., Starinsky, A., Lazar, B.,1981. Low temperature saline waters, Timna, Southern Israel. Report No. M.P. 606/81, Ministry of Energy and Infrastructure and Geological Survey of Israel, Jerusalem.

Bullen, T.D., Krabbenhoft, D.P., Kendall, C., 1996. Kinetic and mineralogic controls on the evolution of groundwater chemistry and ^{87}Sr/^{86}Sr in a sandy silicate aquifer, northern Wisconsin, USA. Geochim. Cosmochim. Acta 60, 1807–1821.

Burg, A., Lifshitz, A., Lomelski, S., Shachar, H., Zuckerman, H., 1999. Hydrological survey for examination of the water potential in the southern Dead Sea and northern Arava Valley. Tahal Report, 99.266, Tel Aviv (in Hebrew).

Burke, W.H., Denison, R.E., Hetherington, E.A., Koepnick, R.B., Nelson, H.F., Otto, J.B., 1982. Variation of seawater ^{87}Sr/^{86}Sr throughout Phanerozoic time. Geology 10, 516–519.

Canfield, D.E., 2001. Biogeochemistry of sulfur isotopes. In: Valley, J.W., Cole, D.R. (Eds.), Reviews in Mineralogy and Geochemistry. The Mineralogical Society of America, Blacksburg, pp. 607–636.

Clark, I., Fritz, P., 1997. Environmental Isotopes in Hydrogeology. Lewis Publishers.

Dansgaard, W., 1964. Stable isotopes in precipitation. Tellus 16, 436–468.

Davis, J.C., Proctor, I.D., Southon, J.R., Caffee, M.W., Heikkinen, D.W., Roberts, M.L., Moore, T.L., Turtletaub, K.W., Nelson, D.E., Loyd, D.H., Vogel, J.S., 1990. LLNL/UC AMS facility and research program. Nucl. Instr. Meth. Phys. Res. B52, 269–272.

Druckman, Y., 1974. The stratigraphy of the Triassic sequence in southern Israel. Bull. Geol. Surv. Israel 64, 1–94.

El-Naser, H., Gedeon, R., 1996. Hydrochemistry and isotope composition of Nubian Sandstone aquifers of Disi-Muawwara area, South Jordan. Isotope Field Applications of Groundwater Studies in the Middle East. International Atomic Energy Agency TECDOC-890, pp. 61–74.

Farber, E., Vengosh, A., Gavrieli, I., Marie, A., Bullen, T.D., Mayer, B., Holtzman, R., Segal, M., Shavit, U., 2004. The origin and mechanisms of salinization of the Lower Jordan River. Geochim. Cosmochim. Acta 68, 1989–2006.

Friedman, I., O'Neil, J.R., 1977. Compilation of stable isotope fractionation factors of geochemical interest. U.S. Geol. Surv. Prof. Paper 440-KK.

Gat, J.R., 1981. Groundwater. In: Technical Report Series No. 210, Stable Isotope Hydrology: Deuterium and Oxygen-18 in the Water Cycle. International Atomic Energy Agency, Vienna, Austria.

Gat, J.R., 1983. Precipitation, Groundwater and Surface Water. Paleoclimates and Paleowater: A Collection of Environmental Isotope Studies. International Atomic Energy Agency, Vienna, Austria.

Gat, J.R., Carmi, I., 1970. Evolution of the isotopic composition of atmospheric water in the Mediterranean Sea area. J Geophys. Res 75, 3039–3048.

Gat, J., Galai, A., 1982. Groundwater of the Arava Valley: an isotopic study of their origin and interrelationships. Israel J. Earth Sci. 31, 25–38.

Gat, J.R., Issar, A., 1974. Desert isotope hydrology: water sources of the Sinai desert. Geochim. Cosmochim Acta 38, 1117–1131.

Gat, J.R., Magaritz, M., 1980. Climatic variations in the Eastern Mediterranean Sea area. Naturwiessenschaften 67, 80–87.

Gavrieli, I., Yechieli, Y., Halicz, L., Spiro, B., Bein, A., Efron, D., 2001. The sulfur system in anoxic subsurface brines and its implication in brine evolutionary pathways: the Ca-chloride brines in the Dead Sea area. Earth Planet. Sci. Lett. 186, 199–213.

Giesemann, A., Joger, H.-J., Norman, A.L., Krouse, H.R., Brand, W.A., 1994. On-line sulphur isotope determination using an elemental analyzer coupled to a mass spectrometer. Anal. Chem. 66, 2816–2819.

Guttman, Y., Burg, A., Lifshitz, A., Lomelski, S., Zuckerman, H., 1999. A flow model for the evaluation of the water potential in the Arava aquifers. Tahal Report, 199.201, Tel Aviv (in Hebrew).

Harrington, G.A., Herczeg, A.L., 2003. The importance of silicate weathering of a sedimentary aquifer in arid Central Australia indicated by very high $^{87}Sr/^{86}Sr$ ratios. Chem. Geol. 199, 281–292.

Harrison, A.G., Thode, H.G., 1957. The kinetic isotope effect in the chemical reduction of sulphate. Trans. Faraday Soc. 53, 1648–1651.

Herut, B., Spiro, A., Starinsky, A., Katz, A., 1995. Sources of sulfur in rainwater as indicated by isotopic $\delta^{34}S$ data and chemical composition, Israel. Atmos. Environ. 29, 851–857.

Issar, A., 1981. The rate of flushing as a major factor in determining the chemistry of water in fossil aquifers in southern Israel. J. Hydrol. 54, 285–296.

Issar, A., Bahat, D., Wakshal, E., 1988. Occurrence of secondary gypsum veins in joints in chalks in the Negev, Israel. Catena 15, 241–247.

Issar, A., Bein, A., Michaeli, A., 1972. On the ancient water of the Upper Nubian Sandstone aquifer in central Sinai and southern Israel. J. Hydrol. 17, 353–374.

Johnson, T.M., DePaolo, D.J., 1994. Interpretation of isotopic data in groundwater systems: model development and application to Sr isotope data from Yucca Mountain. Water Resour. Res. 30, 1571–1587.

Kampschulte, A., Strauss, H., 2004. The sulfur isotopic evolution of Phanerozoic seawater based on the analysis of structurally substituted sulfate in carbonates. Chem. Geol. 204, 255–286.

Kirner, D.L., Taylor, R.E., Southon, J.R., 1995. Reduction in background of microsamples for AMS ^{14}C dating. Radiocarbon 37, 697.

Korte, C., Kozur, H.W., Bruckschen, P., Veizer, J., 2003. Strontium isotope evolution of Late Permian and Triassic seawater. Geochim. Cosmochim Acta 67, 47–62.

Kroitoru, L., 1980. The Hydrogeology of the Nubian Sandstone in Southern Israel (lower Cretaceous). M.Sc. thesis, Tel-Aviv Univ. (in Hebrew).

Levin, M., Gat, J.R., Issar, A., 1980. Precipitation, flood and groundwaters of the Negev highlands: an isotopic study of desert hydrology. In: Proc. Advisory Group Meeting, Arid zone hydrology: investigations with isotope techniques, International Atomic Energy Agency, IAEA-AG-158/1, Vienna, Austria.

McCrea, J.M., 1950. On the isotope chemistry of carbonates and a paleotemperature scale. J. Chem. Phys. 18, 849–857.

Nativ, R., 1987. Permeability distribution in the Jurassic Arad Group in the Negev. Israel J. Earth Sci. 36, 155–160.

Nativ, R., Bachmat, Y., Issar, A., 1987. Potential use of the deep aquifers in the Negev desert, Israel – a conceptual model. J. Hydrol. 94, 237–265.

Nissenbaum, A., 1978. Sulfur isotope distribution in sulfates from surface waters from the Northern Jordan valley, Israel. Environ. Sci. Technol. 12, 962–985.

Patterson, L.J., Sturchio, N.C., Kennedy, B.M., van Soest, M.C., Sultan, M., Lu, Z-T., Lehmann, B., Purtschert, R., El Alfy, Z., El Kaliouby, B., Dawood, Y., Abdallah, A., 2005. Cosmogenic, radiogenic, and stable isotopic constraints on groundwater residence time in the Nubian Aquifer, Western Desert of Egypt. Geochem. Geophys. Geosyst. 6, Q01005. doi:10.1029/2004GC00077.

Plummer, L.N., Prestemon, E.C., Parkhurst, D.L., 1994. An interactive code (NETPATH) for modeling NET geochemical reactions along a flow PATH-version 2.0: U.S. Geol. Surv. Water-Resour. Invest. Report 94-4169.

Puri, S., Appelgren, B., Arnold, G., Aurelli, A., Burchi, S., Burke, J., Margat, J., Pallas, P., 2001. Internationally shared (transboundary) aquifer resources management—their significance and sustainable management: a framework document. IHP-VI, IHP Non-serial Publications in Hydrology SC-2001/WS/40. UNESCO, Paris.

Rosenthal, E., Adar, E., Issar, A.S., Batelaan, O., 1990. Definition of groundwater flow patterns by environmental tracers in the multiple aquifer system of Southern Arava Valley, Israel. J. Hydrol. 117, 339–368.

Rosenthal, E., Issar, A., Kroitoru, L., Gat, J.R., Kronfeld, J., 1981. Hydrogeological inter-relationship between the Judea Group and the Nubian Sandstone aquifers in Sinai and the Negev. Isr. J. Earth Sci. 30, 145–153.

Rosenthal, E., Jones, B.F., Weinberger, G., 1998. The chemical evolution of Kurnub Group paleowater in the Sinai-Negev province – a mass balance approach. Appl. Geochem. 13, 553–569.

Rosenthal, E., Wenberger, G., Berkowiz, B., Flexer, A., Kronfeld, J., 1992. The Nubian sandstone aquifer in central and northern Negev, Israel: delineation of hydrogeological model under conditions of scarce data. J. Hydrol. 132, 107–135.

Sonntag, C., Klitzsch, E., Lohnert, E.P., El-Shazli, E.M., Munnich, K.O., Junghans, C.H., Thorweihe, U., Weistroffer, K., Swailem, F.M., 1978. Paleoclimatic information from deuterium and oxygen-18 in carbon-14 dated North-Saharan groundwaters, Isotope Hydrology, vol. 2. International Atomic Energy Agency (IAEA), Vienna, p. 569.

Southon, J.R., Cafê, M.W., Advise, J.C., More, T.L., Proctor, I.D., Schemata, B., Vogel, J.S., 1990. The new LLNL AMS spectrometer. Nucl. Instr. Meth. Phys. Res. B52, 301–305.

Southon, J.R., Vogel, J.S., Trumbore, S.E., Davis, J.C., Robbers, M.L., Cafê, M.W., Finkel, R.C., Proctor, I.D., Heikkinen, D.W., Berno, A.J., Hornady, R.S., 1992. Progress in AMS measurements at the LLNL spectrometer. Radiocarbon 34, 473–477.

Strebel, O., Bottcher, J., Fritz, P., 1990. Use of isotope fractionation of sulfate-sulfur and sulfate-oxygen to assess bacterial desulfurication in a sandy aquifer. J. Hydrol. 121, 155–172.

Sturchio, N.C., Du, X., Purtschert, R., Lehmann, B.E., Sultan, M., Patterson, L.J., Lu, Z.-T., Müller, P., Bigler, T., Bailey, K., O'Connor, T.P., Young, L., Lorenzo, R., Becker, R., El Alfy, Z.El., Kaliouby, B.El., Dawood, Y., Abdallah, A.M.A., 2004. One million year old groundwater in the Sahara revealed by krypton-81 and chlorine-36. Geophys. Res. Lett. 31, L05503. doi:10.1029/2003GL01923.

Sultan, M., Sturchio, N.C., Hassan, F.A., Hamdan, M.A.R., Mahmood, A.M., El Alfy, Z., Stein, T., 1997. Precipitation source inferred from stable isotopic composition of Pleistocene groundwater and carbonate deposits in the Western Desert of Egypt. Quatern. Res. 48, 29–37.

Veizer, J., 1989. Strontium isotopes in seawater through time. Ann. Rev. Earth Planet. Sci. 17, 141–167.

Veizer, J., Compston, W., 1974. ^{87}Sr/^{86}Sr composition of seawater during the Phanerozoic. Geochim. Cosmochim. Acta 38, 1461–1484.

Veizer, J., Ala, D., Azmy, K., Bruckschen, P., Buhl, D., Bruhn, F., Carden, G.A.F., Diener, A., Ebneth, S., Godde'ris, Y., Jasper, T., Korte, C., Pawellek, F., Podlaha, O.G., Strauss, H., 1999. ^{87}Sr/^{86}Sr, δ^{13}C and d^{18}O evolution of Phanerozoic seawater. Chem. Geol. 161, 59–88.

Veizer, J., Buhl, D., Diener, A., Ebneth, S., Podlaha, O.G., Bruckschen, P., Jasper, T., Korte, C., Schaaf, M., Ala, D., Azmy, K., 1997. Strontium isotope stratigraphy: potential resolution and event correlation. Palaeogeog. Palaeoclim. 132, 65–77.

Vogel, J.S., Nelson, D.E., Southon, J.R., 1987. ^{14}C background levels in an accelerator mass spectrometry system. Radiocarbon 29, 323–333.

Weinberger, G., Rosenthal, E., 1994. The fault pattern in the northern Negev and southern Coastal Plain of Israel and its hydrogeological implications for groundwater flow in the Judea Group aquifer. J. Hydrol. 155, 103–124.

Weinberger, G., Rosenthal, E., Flexer, A., 1991. The subsurface geology of the central and northern Negev with possible implications on the regional groundwater flow pattern. J. Afr. Earth Sci. 14, 155–172.

Yechieli, Y., Bein, A., Halicz, L., 1997. Geochemistry of groundwater in the Central Arava Valley. Isr. Geol. Surv., Rep. GSI/30/96 (in Hebrew).

Yechieli, Y., Starinsky, A., Rosenthal, E., 1992. Evolution of brackish groundwater in a typical arid region: Northern Arava Rift Valley, Southern Israel. Appl. Geochem. 7, 361–374.